# We are IntechOpen, the world's leading publisher of Open Access books
# Built by scientists, for scientists

## 6,900
Open access books available

## 185,000
International authors and editors

## 200M
Downloads

## 154
Countries delivered to

Our authors are among the

## TOP 1%
most cited scientists

## 12.2%
Contributors from top 500 universities

**CLARIVATE ANALYTICS**
**BOOK CITATION INDEX**
**INDEXED**

**WEB OF SCIENCE™**

Selection of our books indexed in the Book Citation Index
in Web of Science™ Core Collection (BKCI)

## Interested in publishing with us?
## Contact book.department@intechopen.com

Numbers displayed above are based on latest data collected.
For more information visit www.intechopen.com

# Applications of Rare Earth Metals in Al-Si Cast Alloys

*Mohamed Gamal Mahmoud, Yasser Zedan,*

*Agnes-Marie Samuel, Victor Songmene, Herebert W. Doty and*

*Fawzy H. Samuel*

## Abstract

The present article reviews a large number of research publications on the effect of mischmetal (MM), rare earth metals (RE), La or Ce, and combinations of La + Ce on the performance of Al-Si cast alloys mainly 319, 356, 380, 413, and 390 alloys. Most of these articles focused on the use of rare earth metals as a substitute for strontium (Sr) as a eutectic silicon (Si) modifier if added in low percentage (< 1 wt.%) to avoid precipitation of a significant amount of insoluble intermetallics and hence poor mechanical properties. Other points that were considered were the affinity of RE to react with Sr., reducing its effectiveness as modifier, as well as the grain refining efficiency of the added RE in any form. None of these articles mentioned the exact composition of the RE used and percentage of tramp elements inherited from the parent ore. Using high purity La or Ce proved to have no effect on the Si shape, size or distribution, in particular at low solidification rates (thick sections). However, regardless the source of the RE, its addition to Sr-modified alloys reduced the modification effect. As for grain refining, apparently a high percentage of RE (> 1 wt.%) is required to achieve a noticeable reduction in grain size, however at the cost of alloy brittleness.

**Keywords:** aluminum alloys, mischmetal, rare earth metals, La, Ce, modification, grain refining, mechanical properties

## 1. Introduction

Silicon is characterized by its low density ($(2.34 \text{ g cm}^{-3})$) coupled with its high hardness (6.5-mohs scale) and low solubility in aluminum matrix which would enhance the alloy wear resistance. The eutectic temperature of Al-11.7% Si alloys is near 577 °C as shown in **Figure 1**, which makes Al-Si alloys easy to cast using different techniques [1–5]. In general, alloys containing Cu and Mg are hardened applying a suitable heat treatable cycle that depends on the thickness of the casting [6–10]. During solidification, the liquid moves along the liquidus line, thus increasing the amount of aluminum, **Figure 2(a)**. At the eutectic temperature, **Figure 2(b)**, almost 50% of liquid has been solidified. As the temperature continues to decrease (577 °C), the rest of the liquid decomposes into solid Al mixed with solid Si but on a finer scale as presented in **Figure 2(c)**.

Soundness of the cast component depends mainly on the ability of the liquid metal to feed interdendritic regions [11]. In the event of low fluidity, shrinkage cavities may occur, as shown in **Figure 3** [12–14], and in the case of automotive
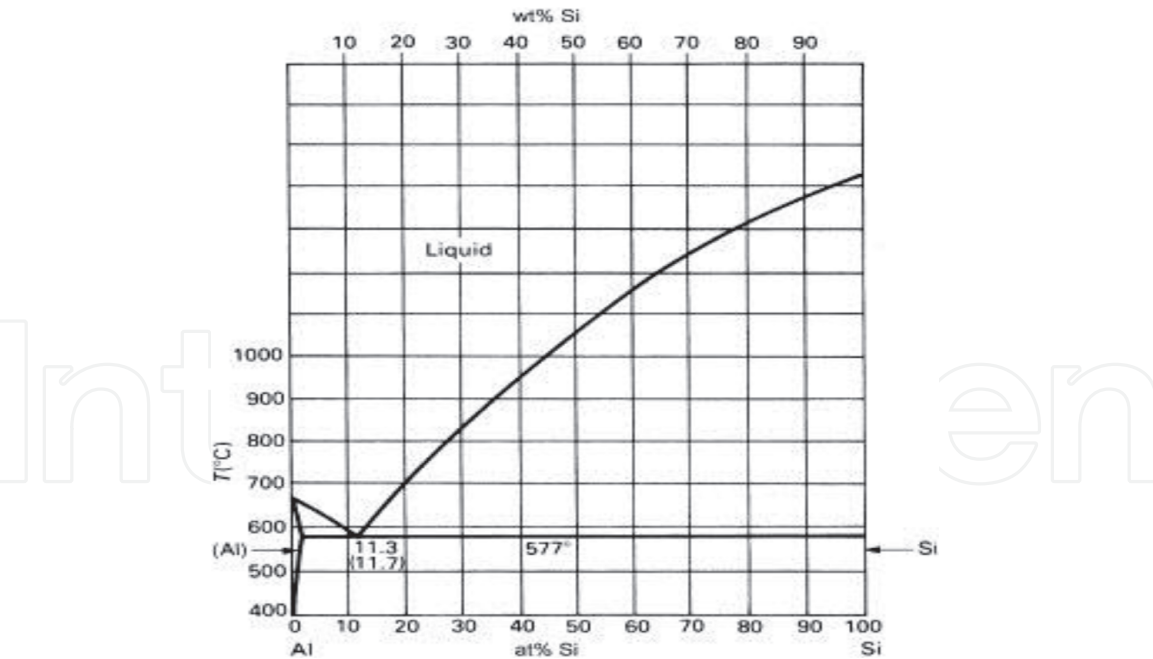
**Figure 1.**
*Al-Si binary diagram [1].*
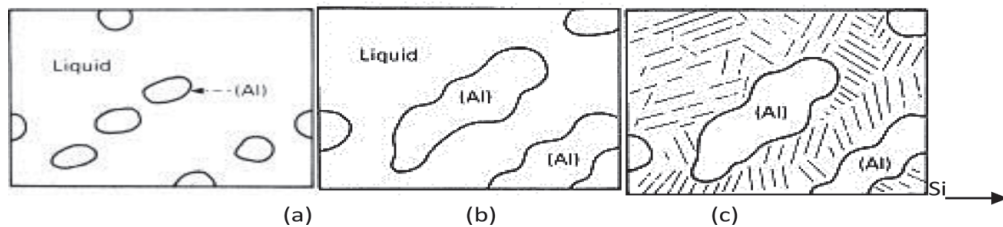


**Figure 2.**
*Progress in liquid to solid during solidification: Start, (b) at eutectic temperature, (c) room temperature [2].*
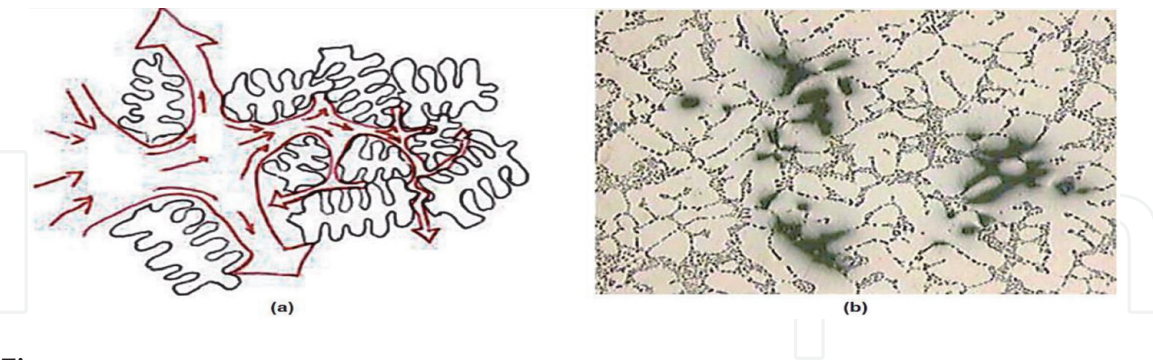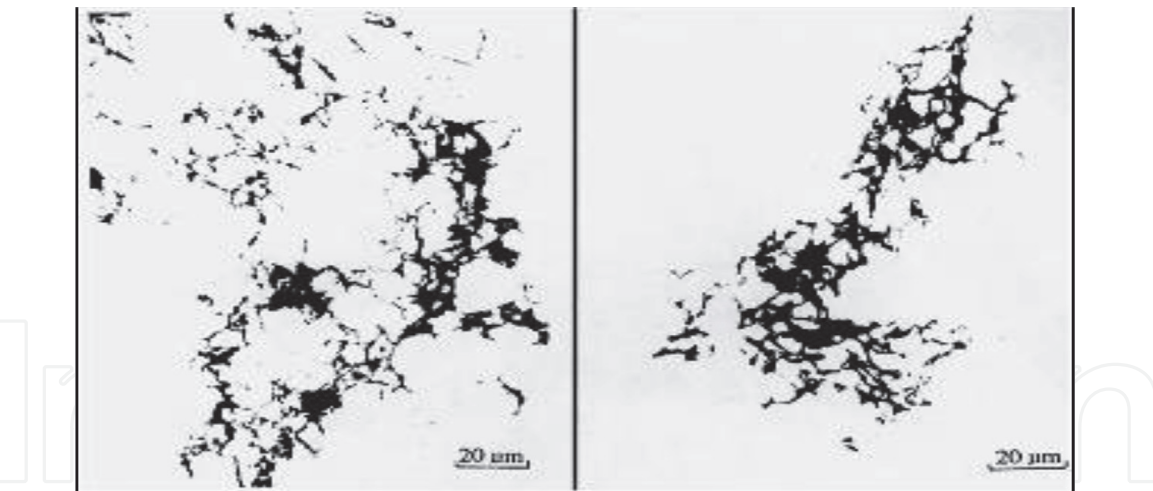


**Figure 3.**
*(a) Schematic diagram showing movement of liquid metal around the dendritic structure, (b) formation if shrinkage cavities [11].*

components, rendering the casting poor pressures tightness. Another point to consider is the introduction of tangled oxide films (bifilms) as shown in **Figure 4**.

Table 1 shows the classification of aluminum cast alloys [14] depending on the main alloying element. The number following the decimal point indicates if the alloys are in the form of castings (.0) or ingots (.1 or .2), whereas **Table 2** depicts the different heat treatment designations for these alloys [15, 16]. The composition of Al-Si alloys that are commonly used in aluminum automotive industries is listed in **Table 3** [17].

High entropy alloys (HEAs) are currently receiving much attention in materials engineering because they have potentially desirable properties [18]. Alloys

**Figure 4.**
*Examples of tangled oxide films in aluminum alloys [13].*

| Alloy Series | Principal Alloying Element |
|---|---|
| 1xx.x | 99.000% minimum Aluminum |
| 2xx.x | Copper |
| 3xx.x | Silicon Plus Copper and/or Magnesium |
| 4xx.x | Silicon |
| 5xx.x | Magnesium |
| 6xx.x | Unused Series |
| 7xx.x | Zinc |
| 8xx.x | Tin |

**Table 1.**
*Classification of aluminum cast alloys.*

| Letter | Details |
|---|---|
| F | As fabricated – no heat treatment |
| O | Annealed – Applies to product which has been heated to produce the lowest strength condition to improve ductility and dimensional stability |
| H | Strain Hardened – Applies to products which are strengthened through cold-working. |
| W | Solution Heat-Treated |
| T | Age hardened alloys - To produce stable other than F, O, or H. The "T" is always followed by one or more digits |

**Table 2.**
*Basic heat treatment designations.*

containing at least 4–5 elements (5–35 at.% concentrations) are considered as HEAs [19]. Research indicates that some HEAs have considerably better strength-to-weight ratios, with a higher degree of fracture resistance, tensile strength, as well as corrosion and oxidation resistance than conventional alloys. The research investigations on the Al-Si alloys being reviewed here also focus on achieving the same characteristics.

In this review, the microstructures and mechanical properties of aluminum alloys containing different rare earth element additions are discussed, mainly 319,

| Alloy | Elements (wt. %) | | | | | | |
|---|---|---|---|---|---|---|---|
| | Method(b) | Si | Cu | Mg | Fe | Zn | Others |
| 319.0 | S, P | 6.0 | 3.5 | <0.10 | <1.0 | <1.0 | |
| 332.0 | P | 9.5 | 3.0 | 1.0 | 1.2 | 1.0 | |
| 355.0 | S, P | 5.0 | 1.25 | 0.5 | <0.06 | <0.35 | |
| A356.0 | S, P | 7.0 | <0.20 | 0.35 | <0.2 | <0.1 | |
| A357.0 | S, P | 7.0 | <0.20 | 0.55 | <0.2 | <0.1 | 0.05 Be |
| 380.0 | D | 8.5 | 3.5 | <0.1 | <1.3 | <3.0 | |
| 383.0 | D | 10.0 | 2.5 | 0.10 | 1.3 | 3.0 | 0.15 Sn |
| 384.0 | D | 11.0 | 2.0 | <0.3 | <1.3 | <3.0 | 0.35 Sn |
| 390.0 | D | 17.0 | 4.5 | 0.55 | <1.3 | <0.1 | <0.1 Mg |
| 413.0 | D | 12.0 | <0.1 | <0.10 | <2.0 | — | |
| 443.0 | S, P | - 5.25 | <0.3 | <0.05 | <0.8 | <0.5 | |

*S = sand casting, P = permanent mold casting, D = die casting.*

**Table 3.**
*Composition of Al-Si based cast alloys commonly used in automotive components [17].*

356, 380, 411, and 390 alloys which constitute alloys widely used in automotive components. A number of scientific investigations are reported in the literature on the effects of rare earth elements and mischmetal (MM), which is a mixture of rare earth (RE) elements found in abundance in nature with Cerium (Ce) and Lanthanum (La) together comprising approximately 90% of mischmetal. The RE metals investigated include Cerium (Ce), Lanthanum (La), Yttrium (Y) [20–25], Erbium (Er) [26–30], Neodymium (Nd) [31–35], Ytterbium (Yb) [36–40], Samarium (Sm) [41–42], Scandium (Sc) [43–47], Europium (Eu) [48, 49], and Gadolinium (Gd) [50]. Among these, the effects of MM, Ce, La and mixed additions of Ce and La are reviewed.

## 1.1 Effects of Mischmetal (MM) additions

The effects of small amounts of mischmetal (MM) on the dendrite arm spacing, and the Brinell hardness of Al-1.0% Mg-0.5% Si alloy were investigated by Young et al. [51]. Their results showed that in the range of 0.5–4.0 wt.% MM the hardness increased by more than 30% and the dendrite arm spacing decreased from 50 μm to 18 μm. Ravi et al. [52] analyzed the mechanical properties and microstructure of cast Al-7Si-0.3 Mg (LM25/356) alloy and reported that addition of above 1.0 wt.% of MM lowered the YS, UTS and percent elongation, with an increase in the Brinell hardness. The mechanical properties decreased due to the formation of Ce and La hard intermetallic compounds in the matrix and consumption of a certain amount of Mg in their formation, which reduced the strengthening constituent $Mg_2Si$ formed, contributing to the observed decrease. The yield strength (YS), ultimate tensile strength (UTS), and pct elongation of the Al-7Si-0.3 Mg alloy (in the T6 condition) decreased with the increase in Fe content (from 0.2 to 0.6 pct), as shown in **Figure 5**.

The microstructure and thermal analysis of Al-21 wt.% Si alloys with MM addition were discussed by Chang et al. [53, 54]. According to the authors, addition of 2.0 wt.% MM leads to a morphological change in the primary Si crystals from star-like to polyhedral shape [55] as displayed in **Figure 6**. The thermal analysis results
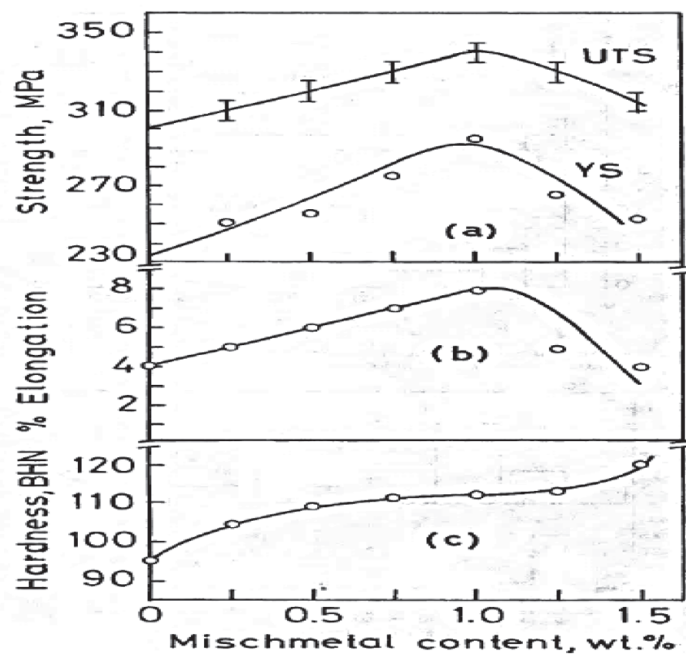
**Figure 5.**
*Mechanical properties of the LM 25 alloys (−T6 condition) containing Fe and Mischmetal [52].*
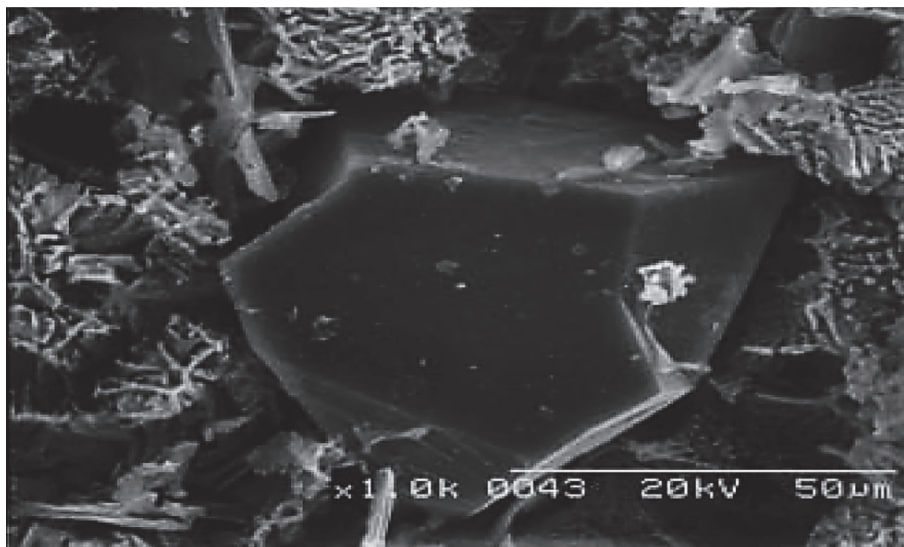


**Figure 6.**
*Scanning electron micrograph of the deep etched Al-21% Si-3% RE alloy. The RE modified primary Si shows typical polyhedral shape [54].*

revealed that addition of 3.0 wt.% of MM leads to depressions of 12-17 °C in the primary Si reaction temperature and 2–7 °C in the eutectic Si temperature. Increasing the level of MM additions to in situ Al-15Mg$_2$Si composite alloy leads to: (i) a reduction in the size of Mg$_2$Si particles, (ii) a change in the morphology of eutectic Mg$_2$Si from fibrous to flake like, and (iii) formation of RE-containing compounds in the form of Al$_{11}$RE$_3$ [56].

Ravi et al. [57] studied the effect of 1.0 wt.% MM additions on the microstructural characteristics and the room and elevated temperature tensile properties of Al-7Si-0.3 Mg (LM 25/356) alloy containing excess iron up to 0.6 wt.%. The results showed that:

    i. Alloys with Fe contents ranging from 0.2 to 0.6 wt.%, exhibit grain refinement and partial modification of the eutectic silicon and the finer

intermetallic compounds formed with Ce, La, and other elements, thereby improving the strength as well as the ductility of the alloy relative to the same alloys without MM addition.

ii. Alloys containing 0.6 wt.% Fe led to the formation of fine and fibrous shaped intermetallic compounds containing Fe and Si, which reduced the effective amount of Fe available for formation of β and π phases, thereby reducing the size and volume of Fe-containing intermetallics, which, in turn, reduced the deleterious effect of Fe and improved the alloy strength and ductility.

Wan et al. [58] found that up to 1.0 wt%, MM addition refined the grain size of cast Al-Cu-Mg-Si alloy and changed the eutectic Si morphology from needle-like and laminar to a granular type. Also, with the increase of the MM level, the tensile strength and elongation of the alloy first increased and then began to decrease. Alloy with 0.7 wt.% MM exhibited the highest mechanical properties. In another study, Chong et al. [59] studied the combined effects of P and MM on the microstructure and mechanical properties of hypereutectic Al-20%Si alloy. It was observed that, in general, alloys with the addition of 0.08% P and 0.6% MM exhibited highest mechanical properties and had the optimal microstructure compared to the alloy with no addition; refinement of the primary Si particles from 66.4 μm to 23.3 μm, and the eutectic silicon from 8.3 μm to 5.2 μm, was also noted. With respect to the mechanical properties, the ultimate tensile strength improved from 256 MPa to 306 MPa, and the ductility increased from 0.35% to 0.48%. **Figure 7** shows the average primary Si size of the tested alloys with different P contents.

According to El Sebaie et al. [60–64] the presence of MM in unmodified and Sr-modified A319.1, A356.2 and A413.1 Al-Si casting alloys led to the following observations:

i. In general, the hardness values of the as-cast alloys were higher at high cooling rates than at low cooling rates. With MM, the hardness decreased at both solidification rates. **Figure 8** shows the hardness values obtained for these alloys after different aging treatments.
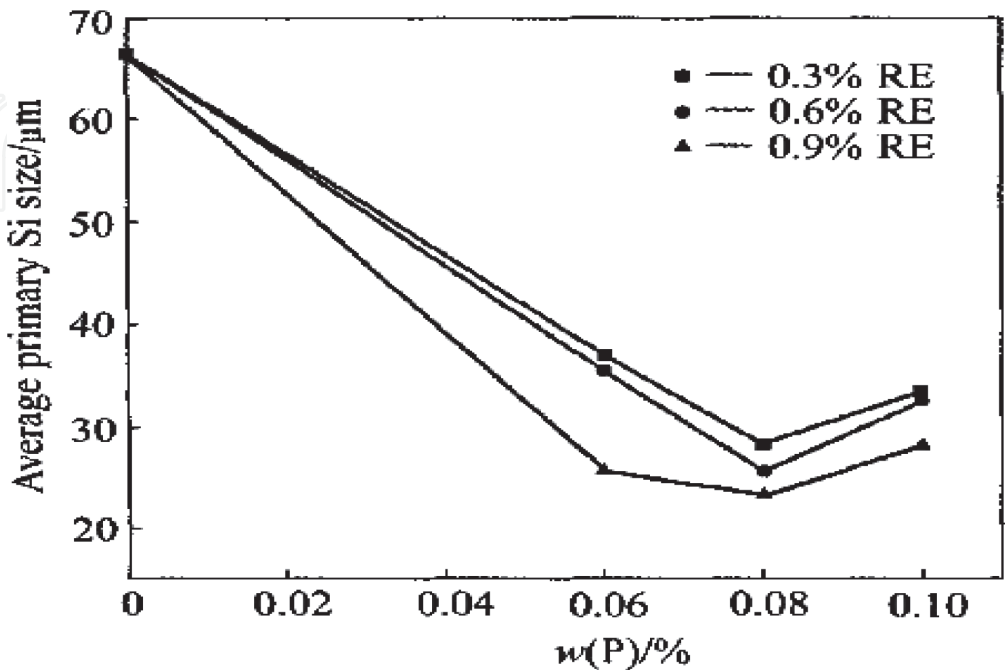


**Figure 7.**
*Effect of P content on primary Si size of Al-20%Si alloys under same RE content condition [59].*

ii. In the case of non-modified alloys MM addition resulted in partially modified eutectic silicon particles. This effect was more pronounced in the A413.1 and A319.1 alloys, compared to A356.2 alloy.

iii. The effect of MM as a modifier is more effective at high cooling rate (corresponding to DAS ~ 40 μm) than at the low cooling rate (DAS ~ 120 μm) for all the as-cast non-modified alloys.

iv. MM-containing intermetallic phases were observed at high and low cooling rates, each exhibiting a specific Ce/La ratio and morphology. Many of these MM-containing intermetallic phases were found to contain Sr., which confirmed the interaction of MM with Sr. – see **Figure 9** and Appendix A.

Combined addition of MM and Mn is an effective way to improve the strength of A390 alloy at elevated temperature by 25% [65]. Other studies by Zhu et al. [66, 67] reported the effects of 0.1–1.0 wt.% Ce-based MM additions on the microstructure, tensile properties and fracture behavior of as-cast and T6-treated A356 alloys. The main findings from their work are listed below for the specified conditions.

*1.1.1 MM-modified as-cast A356 alloys*

MM-containing intermetallic compounds cannot act as potential nucleate sites for the primary α-Al phase.

i. The modification effect of MM depends on the addition level. Minor additions of MM (less than 0.2 wt.%) result in partial modification, while more than 0.3 wt.% MM leads to full modification.

ii. The fracture path goes through the interdendritic region composed of eutectic silicon and MM-containing intermetallic compounds.
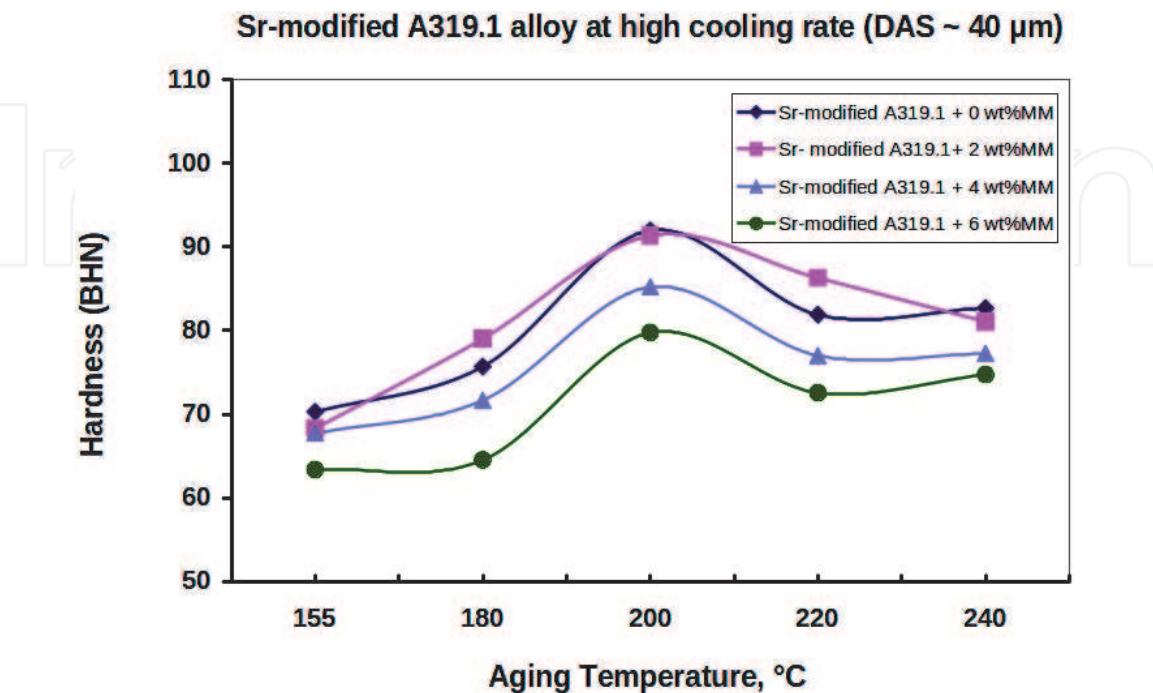


**Figure 8.**
*Effect of mischmetal additions and aging temperature on the hardness of A319.1 alloys solidified at high solidification rates (DAS ~ 40 μm of Sr-modified conditions [63].*
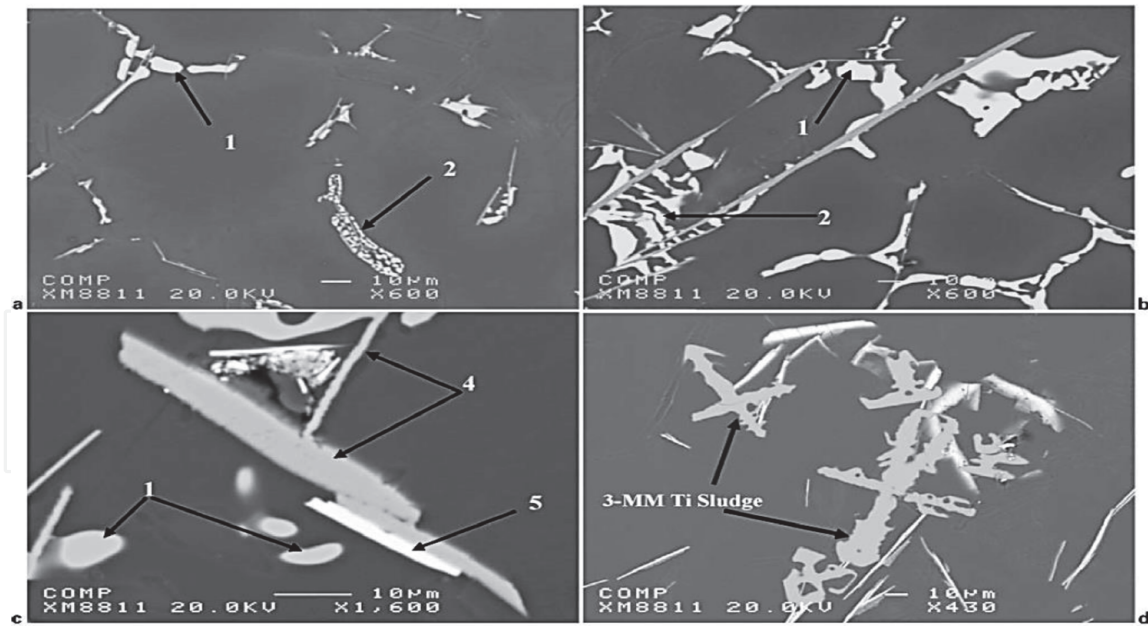
**Figure 9.**
*Backscattered images of A319.1 alloy samples containing (a, b) 0 wt-% and (c, d) 6 wt-%MM depicting intermetallic phases observed under high cooling rate conditions (S: Sr. modified; T: Heat treated samples) [64].*
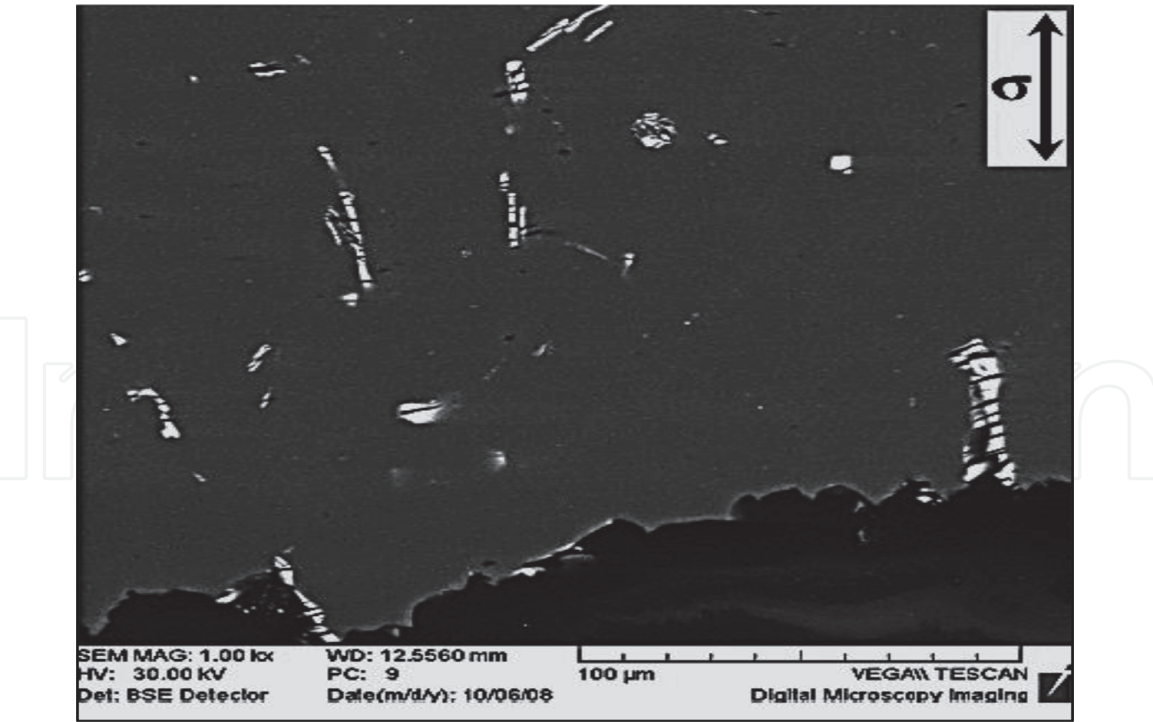
### 1.1.2 MM-modified T6-A356 alloys

T6 heat treatment has great influence on the spheroidization of eutectic silicon particles in MM-modified A356 alloys than that in the unmodified alloys.

i. The UTS, YS, and %EL of the T6-treated A356 alloys with and without modification are improved due to the spheroidization of eutectic silicon particles and $Mg_2Si$ precipitation hardening.

ii. SEM images show that the MM-modified T6 A356 alloy undergoes ductile fracture. It is worth noting that the eutectic silicon and MM-containing intermetallic particles provide the weak locations for initiation of the fracture as displayed in **Figure 10**.

The effects of different addition levels (0.0–1.0 wt.%) of La-based MM and heat treatment on the microstructure and tensile properties of two different sections of Al-Si casting alloy A357 were studied by Mousavi et al. [68–70]. Optimum recommended levels of MM are 0.1 wt.% and 0.3 wt.% for thin and thick sections of the casting, respectively. Examination of the microstructure at high level of MM (0.5 wt.%) exhibited the precipitation of a new AlSiLa intermetallic phase as shown in **Figure 11**.

The results of Jiang et al. [71] on the microstructure, tensile properties and fracture behavior of as-cast and T6 A357 alloy revealed that addition of MM reduced the size of the primary α-Al dendrites i.e., the SDAS value, and also improved the eutectic Si particle morphology. Accordingly, the MM-modified A357 alloy exhibited improvement in the tensile properties, particularly the elongation, in the T6-treated condition. The fracture surface of the tensile-tested sample of the unmodified alloy showed a clear brittle fracture, whereas that of the MM-modified A357 alloy exhibited dimple rupture and cracked eutectic Si particles, resulting in superior ductility. The results of Zhang et al. [72, 73] demonstrated that the AlTiB-MM addition to A356 alloy provided the most effective and synergetic grain size refinement compared to individual AlTiB or MM additions. Also, the properties of

**Figure 10.**
*Fracture surface parallel to the tensile direction of the T6-A356 alloys modified by 0.5 wt.% MM showing intercrystalline crack of RE-containing intermetallic compounds at the fracture surface [67].*
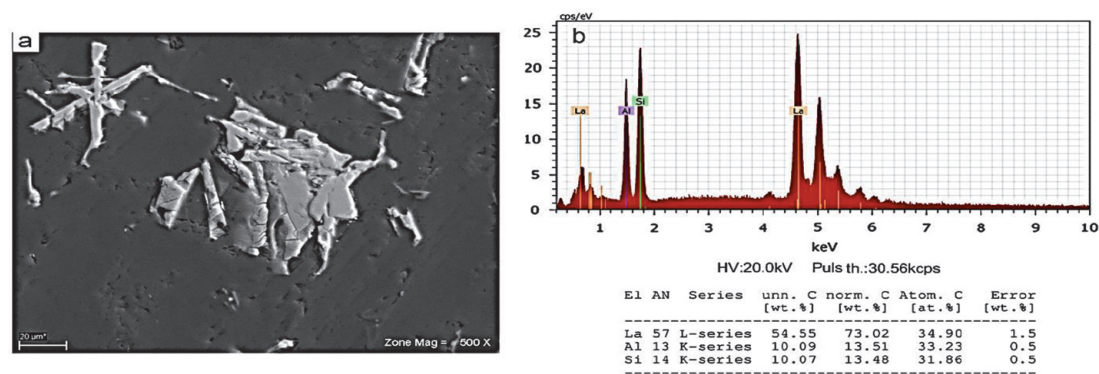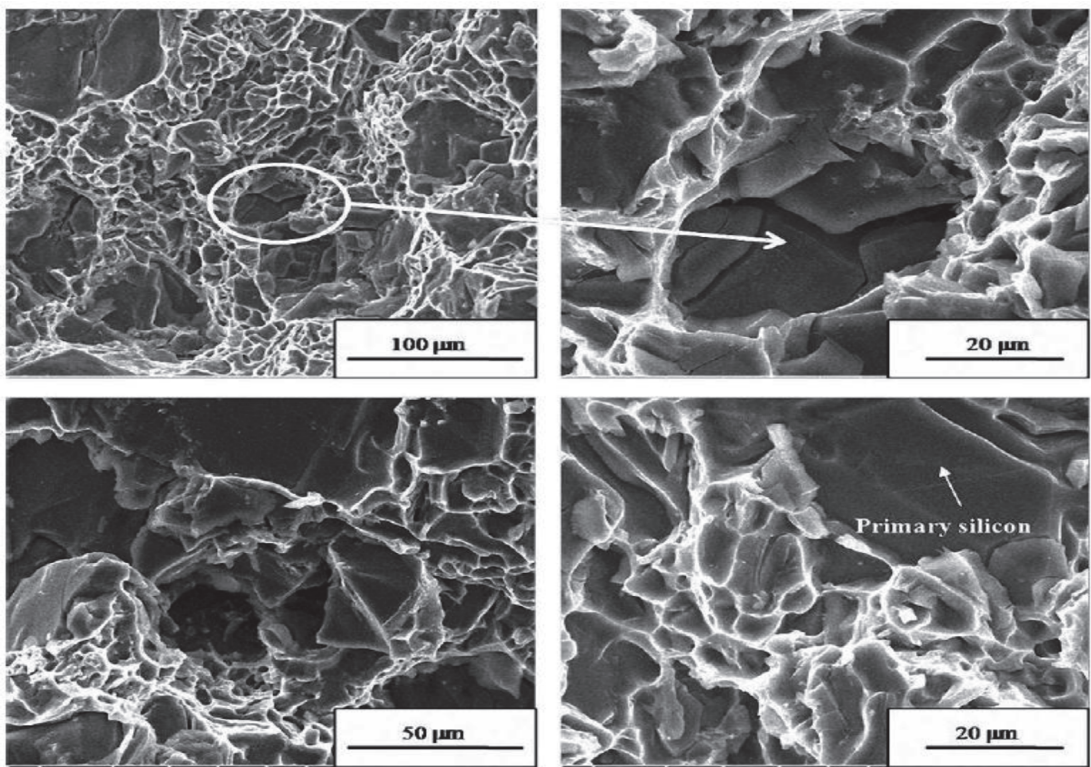


**Figure 11.**
*(a) SEM photograph of Al–Si–La compound intermetallic in A357 alloy with 0.5 wt% mischmetal casting in thick section mold and (b) EDS spectrum showing the distribution of Al, Si and La in the intermetallic [70].*

A356 alloy wheel refined by the AlTiB-MM were improved significantly. The tensile strength, yield strength, and elongation of the wheel spokes improved by approximately 11.3%, 10.8% and 44.1%, respectively.

Dang et al. [74] investigated the effects of the use of rare earth (RE) in the form of Al-10% RE master alloy (a mixture of Ce and La) and pouring temperature (1124 K through 1524 K in increments of 100 K) on the microstructure and mechanical properties of T6-treated Al-25%Si alloy. The authors observed that for the unmodified alloy, the primary Si morphology was transformed from platelets to fine polyhedral form, and the average size decreased with increase in pouring temperature (from 125 µm at 1124 K to ~62 µm at 1524 K). With a 1.2 wt.% RE addition, the primary Si exhibited a small blocky morphology, with an average particle size of 47 µm. In addition, the study showed that T6 MM-Al-25%Si alloy exhibited an improvement in the mechanical properties compared to the unmodified alloy, where the maximum tensile strength and elongation (208.3 MPa and 1.01%) were obtained for the sample modified with 1.2 wt.% RE followed by

the T6 heat treatment. Tensile fracture exhibited three stages: microcrack initiation, crack coalescence, and quick crack propagation as shown in **Figure 12**.

According to Mahmoud et al. [75, 76], depending upon the amount of added Ti, two RE-based intermetallics can be formed: (i) a white phase, mainly platelet-like (approximately 2.5 μm thick), that is rich in RE, Si, Cu, and Al, and (ii) a second phase made up of mainly gray sludge particles (star-like) branching in different directions. The gray phase is rich in Ti with some RE (almost 20% of that in the white phase) with traces of Si and Cu. There is a strong interaction between RE and Sr., leading to a reduction in the efficiency of Sr. as a eutectic Si modifier, causing particle demodification. **Figure 13(a)** shows the actual morphology of the white phase which is likely to be thin platelets about 2.5 μm thick. The morphology of the gray sludge is well illustrated in **Figure 13(b)** exhibiting the branching of the gray phase particles in different directions.



**Figure 12.**
*The fracture morphology of Al-25% Si alloy in: (a) and (b) 1.2% RE, (c) and (d) 1.2% RE + T6 heat treatment [74].*
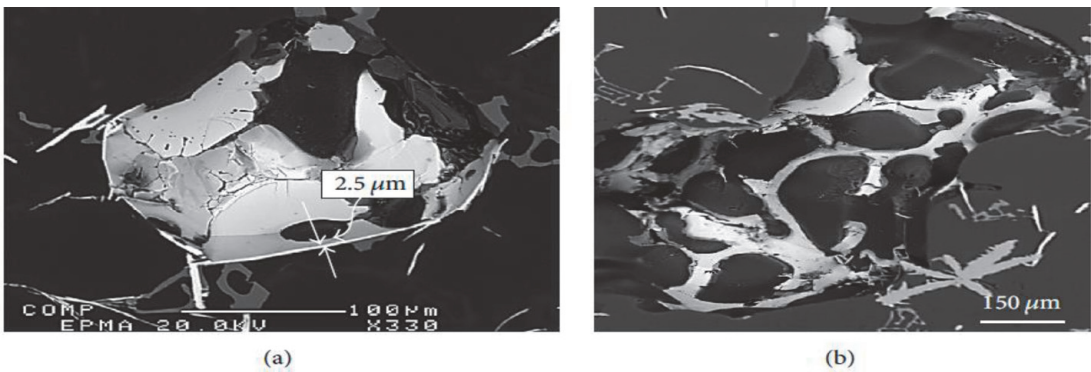


**Figure 13.**
*RE-based intermetallic phases: (a) platelet-like phase; the two straight arrows pointing towards each other simply highlight the thickness of the platelet-like phase and the curved arrow that links the label 2.5 μm to the platelet indicates the actual thickness, (b) the gray sludge phase [76].*

## 1.2 Effects of cerium additions

The results arising from the investigations of Song et al. [77, 78] showed that individual addition of 0.3%Ce or 0.2%Ti to Al-Cu-Mg-Ag alloys can decrease the grain size of the as-cast alloy, increase the nucleation rate of the Ω (metastable Al$_2$Cu) phase, inhibit the growth of the Ω phase during aging, and thereby increase the volume fraction and decrease the spacing of the Ω phase. Based on these microstructural observations, the yield strength and tensile strength of the alloy are increased. However, combined addition of Ce and Ti led to the formation of (Ce, Ti)-containing intermetallic compounds and increased the grain size during casting, with no influence on the nucleation and growth of the Ω phase during aging. The alloy containing both Ce and Ti had a relatively lower Vickers hardness and strength compared to the alloy containing individual additions of Ce or Ti. In another research, Song et al. [79] reported that Ce improved the thermal stability of the Ω phase by decreasing the diffusion velocity of the Cu atoms, and hence decreasing the coarsening speed of the phase, as well as through the aggregation of Ce atoms at the Ω phase/Al matrix interface, increasing the energy barrier for the thickening of the Ω phase plates which coarsen through a ledge nucleation mechanism. The strength of the Al-Cu-Mg-Ag alloy is improved, as a result.

The results on the effects of different levels of Ce additions on the microstructure, thermal behavior and mechanical properties of hypereutectic AlSi17CuMg alloy illustrated that addition of Ce (up to 1.0 wt.% Ce) can achieve refinement of the primary and eutectic silicon morphology. In general, alloy containing 1.0 wt.% Ce exhibited the best results with respect to the microstructural and strength properties. It was also observed that with 1.0 wt.% Ce, the alloy produced the highest reduction in the liquidus temperature from 686.6 °C to 591.9 °C. [79].

The eutectic silicon modification in A356 alloy modified with 1.0 wt.% Ce was greatly improved [80]. However, the thermal analysis revealed that there is no direct relation between the eutectic growth temperature and silicon modification. The microstructural characterization showed that two kinds of Ce-containing intermetallic phases were found, including Ce-23Al-22Si and Al-17Ce-12Ti-2Si-2 Mg (in wt.%). While the ductility of the Ce-modified alloys was enhanced for Ce additions of 0.6 wt.% and above, there was no positive effect on the ultimate tensile strength; this was attributed to the formation of the Al-17Ce-12Ti-2Si-2 Mg phase which reduced the amount of free Mg available for precipitation of the Mg$_2$Si strengthening phase.

The effects of various concentrations of Ce (0.0, 0.01, 0.02, 0.05 and 0.1 wt.%) on the solidification and mechanical properties of AA A360 (Al-10%Si-0.5%Mg) alloy were reported by Voncina et al. [81]. The results showed that the solidus temperature decreased with increasing Ce addition. The eutectic ($\alpha_{Al}$ + Mg$_2$Si) temperature also decreased with Ce addition. It was found that the precipitation enthalpy decreased with the Ce addition, while precipitation occurred more rapidly and intensively, indicating increased reaction kinetics. Mechanical properties like tensile strength and hardness also increased with the Ce addition, where the hardness of the investigated alloy could be attributed to the phase composed of Al, Ce, Mg and Si. The precipitation enthalpy also decreased with increasing Ce addition and increased with increasing cooling rate as determined from simple DSC analysis, as shown in **Figure 14**. It was anticipated that Ce in A360 alloy decreases the activation energy for the precipitation of the Mg$_2$Si phase and consequently precipitation enthalpy.

It is worth noting that in another study Voncina et al. [82] reported that addition of Ce to A380 alloy led to a change in the morphology of eutectic Al$_2$Cu phase from "crumbled" to fully formed (finer eutectic-like to blocky form) and caused the
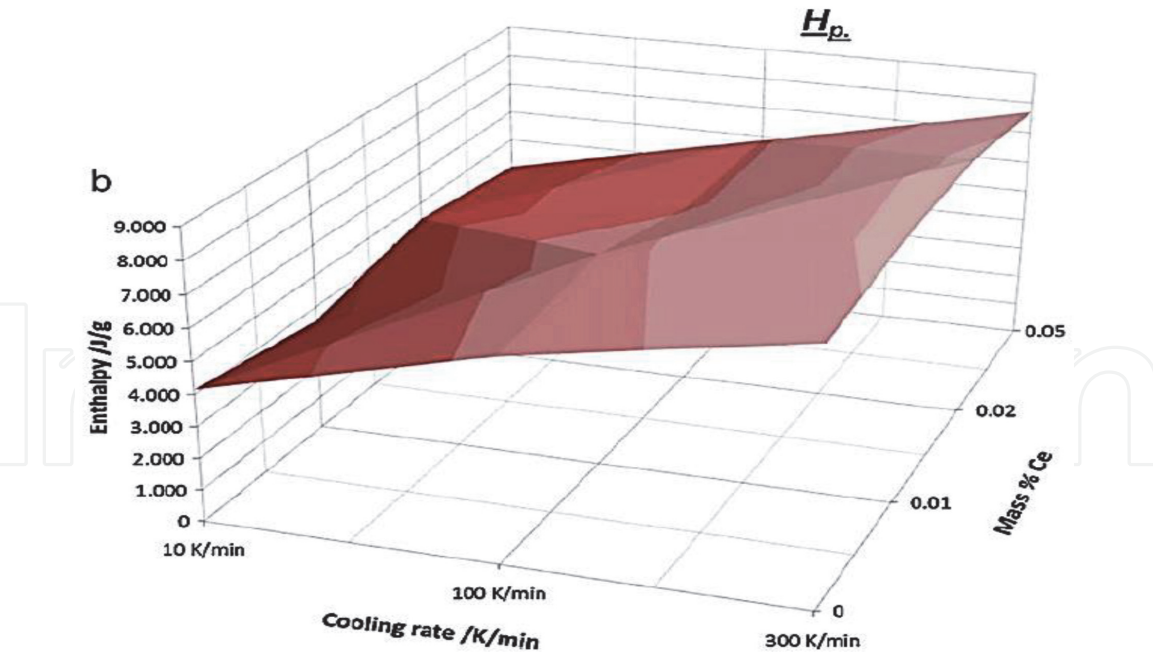
**Figure 14.**
*Precipitation enthalpy regarding the Ce addition and cooling rate at heating DSC curves.*
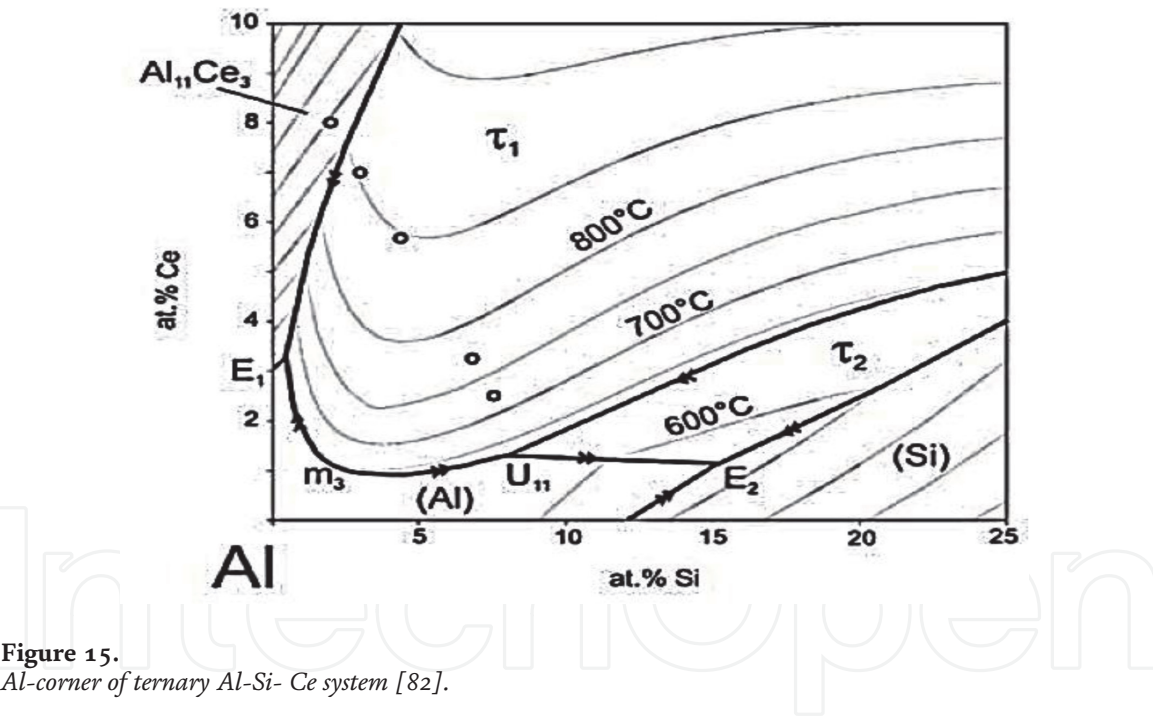


**Figure 15.**
*Al-corner of ternary Al-Si- Ce system [82].*

formation of small primary crystals of $\alpha_{Al}$ which resulted in grain refining of the alloy. A needle-shaped AlCeCuSi phase ($Al_9Ce_2Cu_5Si_3$) was also detected. The solidification of hypoeutectic Al-Si alloys with Ce addition can be described by the Al-corner of ternary system Al-Si-Ce (**Figure 15**).

Effects of Ce-Sr interaction on the nucleation of primary α-Al phase dendrites in hypoeutectic Al-7%Si-Mg cast alloy were examined by Chen et al. [83]. It was found that with addition of Ce and Sr., the grain size of the dendritic α-Al phase becomes well refined, decreasing from 150 μm to 90 μm, and is attributed to the exponential increase in nucleation frequency ($10^{24}$), compared to the unmodified alloy, and restricted growth. Increasing the Ce level (0, 0.3, 0.5, 0.8 and 1 wt.%) in Al-20%Si alloy would cause a significant refinement of the primary Si crystals with the change in the morphology of the eutectic Si phase from coarse platelet like to a fine fibrous

structure [84]. Accordingly, the ultimate tensile strength (UTS) and elongation (% El) increased by 68.2% and 53.1%, respectively, as a result of these effects.

Ye et al. [85] investigated the influence of Ce content (0.2% and 0.4 wt.%) on the impact properties and microstructures of 2519A aluminum alloy, a new version of 2519 alloy (with a higher Cu/Mg ratio) used for armor material. Based on the results of their research, it was found that 0.2 wt.% Ce addition leads to an increase in the volume fraction of the precipitation phase, in addition to a more dispersive and homogeneous distribution of finer θ' ($Al_2Cu$) precipitates, which result in improving the ability of the alloy for absorbing impact energy. Formation of $Al_8Cu_4Ce$ phase which is thermally stable at high temperature is also expected to enhance the high temperature mechanical properties of the alloy. Yii et al. [86] reported that the addition of Ce in the Al-20%Si alloys refined the Si primary phase as the Ce additions were increased. The results also showed that addition of Ce in the range of 0.46 to 2.24 wt.% led to the formation of fine cells dispersed in the Al-matrix. These cells consisted of a mixture of eutectic Si particles and Ce-containing intermetallic phases ($Al_3Ce$ and $CeAl_{1.2}Si_{10.8}$). The amount of the intermetallic phases increased with increasing Ce addition.

Promising scientific investigations were made by Ahmad and coworkers [87, 88] on the influence of Ce on the microstructure of a commercial Al-11%Si-Cu-Mg eutectic cast alloy (ADC12). The main findings from their studies are summarized below.

i. The addition of Ce to ADC12 alloy leads to improvement in the Si particles modification and reduces the Si particle size by 62% [87].

ii. Cooling rate has no significant effect in the 1.5 wt.% Ce-modified ADC12 alloy, compared to the base alloy and this may be attributed to the formation of intermetallic phases.

iii. Investigation of the Al-Si eutectic phase using the thermal analysis technique showed that addition of Ce had a significant effect on the nucleation, growth, and minimum temperatures of Al-Si, and decreased as the Ce concentration increased; refinement of the Si structure was observed up to 1.0 wt.% Ce. In addition, the growth and nucleation temperatures of the Al–Cu phase, which is the last phase to solidify, also increased with increasing level of Ce. The formation of Ce-containing intermetallic compounds such as Al-Si-Ce and Al-Si-Cu-Ce affected the degree of Si modification [88] - **Figure 16** and **Table 4**.

iv. Ce addition refined the secondary dendrite arm spacing (SDAS) by approximately 36%. In addition, the tensile strength and quality index of Al-11%Si-Cu-Mg increased to 237.6 MPa and 265 MPa, respectively, after the addition of 0.1 wt.% Ce.

Effect of solidification rate and rare earth metal addition on the microstructural characteristics and porosity formation in A356 alloy was investigated by Mahmoud et al. [89]. According to the atomic radius ratio, $\gamma La/\gamma Si$ is 1.604 and $\gamma Ce/\gamma Si$ is 1.559, theoretically, which shows that Ce is relatively more effective than La. These findings confirm that Sr. is the most dominating modification agent. Interaction between rare earth (RE) metals and Sr. would reduce the effectiveness of Sr. Although modification with Sr. causes the formation of shrinkage porosity, it also reacts with RE-rich intermetallics, resulting in their fragmentation. **Figure 17** reveals the distribution of La, Ce, and Sr. in RE-rich platelets, which explains the
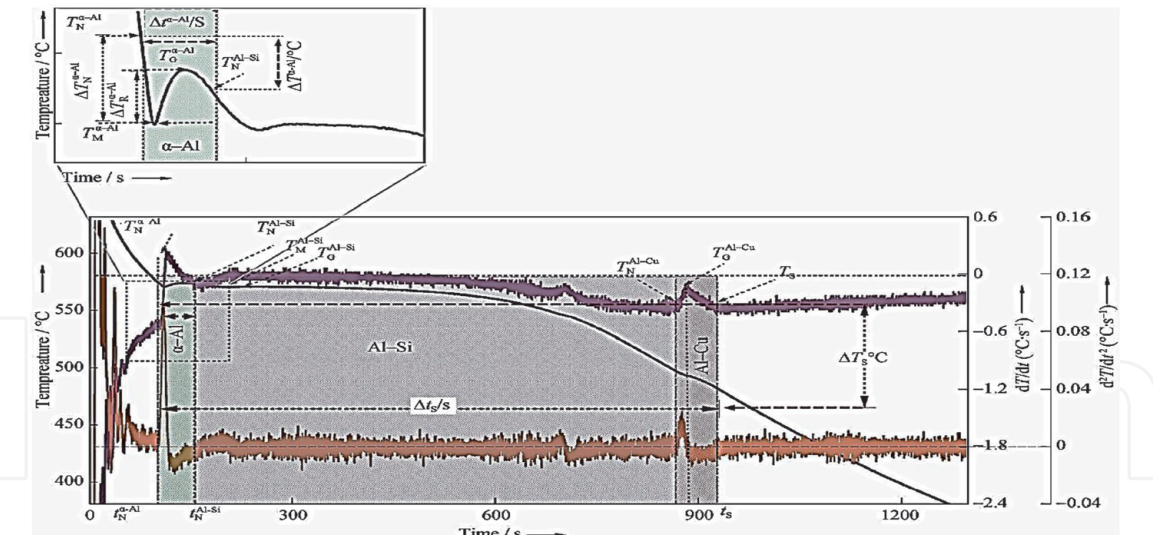
**Figure 16.**
*Cooling curve and the first and second derivative of the 0.1 wt% Ce-containing alloy with characteristic parameters and α-Al phase arrest regions, showing points of interest [88].*

| Parameter | Description |
|---|---|
| $T_N^{\alpha-Al}/°C$ | Nucleation temperature of α-A1 (onset of a-A1 phase) |
| $T_M^{\alpha-Al}/°C$ | Minimum temperature of α-A1 |
| $T_G^{\alpha-Al}/°C$ | Maximum growth temperature of α-A1 |
| $T_R^{\alpha-Al}/°C$ | Recalescence temperature = $T_G^{\alpha-Al} - T_M^{\alpha-Al}$ |
| $T_N^{\alpha-Al}/°C$ | Nucleation undercooling temperature = $T_N^{\alpha-Al} - T_M^{\alpha-Al}$ |
| $\Delta T^{\alpha-Al}/°C$ | Solidification temperature range of α-A1 phase = $T_N^{\alpha-Al} - T_N^{Al-Si}$ |
| $T_N^{Al-Si}/°C$ | Nucleation temperature of Al-Si (end of α-A1 phase) |
| $T_s/°C$ | Solidus temperature (end of solidification) |
| $t_s/s$ | Solidus time (end of solidification) |
| $\Delta T_s/°C$ | Total temperature range = $T_N^{\alpha-Al} - T_s$ |
| $\Delta t_s/s$ | Total temperature range = $t_N^{\alpha-Al} - t_s$ |

**Table 4.**
*Solidification characteristic parameters identified during solidification of the α-A1 phase and at the end of solidification.*

partial modification of the surrounding Si particles as less Sr. is available for modification of the eutectic Si.

## 1.3 Effects of lanthanum additions

It is inferred from the work of Mahmoud et al. [90] using high purity (99.5%) lanthanum or cerium, that La and Ce have more or less the same effect on the microstructures, with the La- and Ce-containing intermetallics displaying similar morphologies. Regardless of the alloy composition, an addition of 150 ppm Sr. or 0.2% RE results in improving the UTS by 25–52% in the T6 condition, with a decrease in ductility from 3% to 2.1%. The addition or RE metals (La + Ce) up to 3 wt.% leads to an increase in the freezing range through an increase in the melting point of the non-modified alloys, with decrease in the Al-Si eutectic temperature, by 12 °C and 8 °C, respectively, at 3 wt.% addition, **Figure 18**. The authors
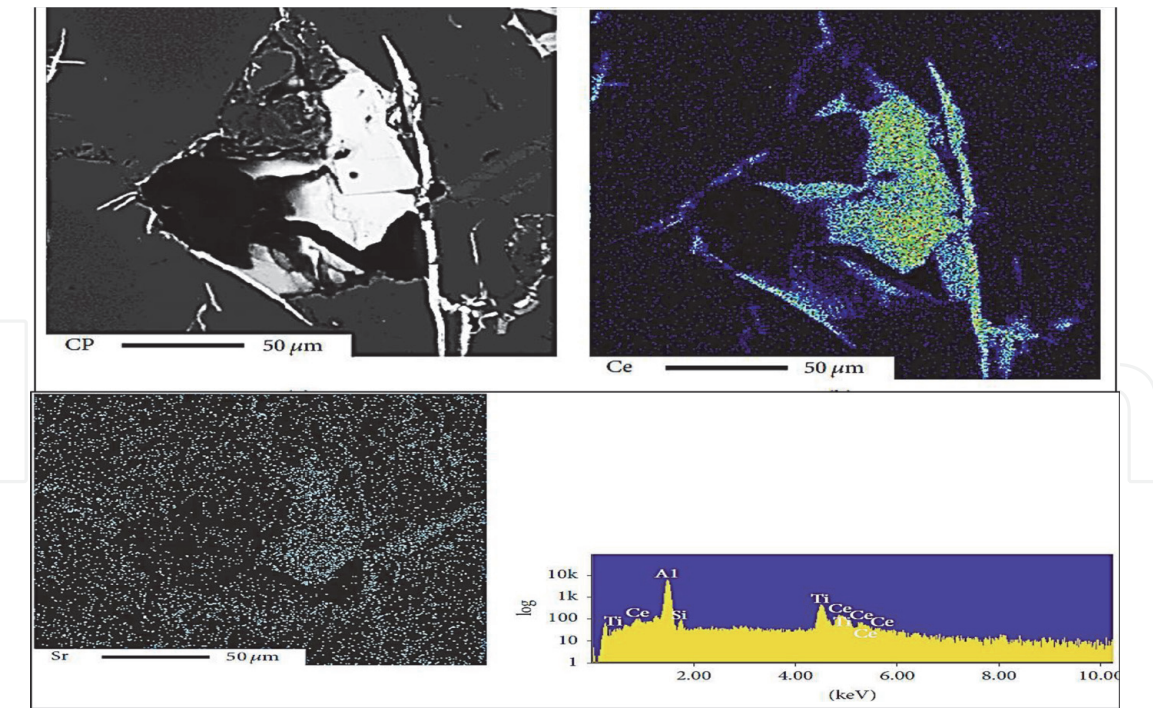
**Figure 17.**
*(a) Backscattered electron image showing Ce-rich platelets in Sr-modified A356 alloy containing 1.025% wt.% Ce, and elemental distribution of (b) Ce, (c) Sr., and (d) EDS spectrum corresponding to (a) [89].*
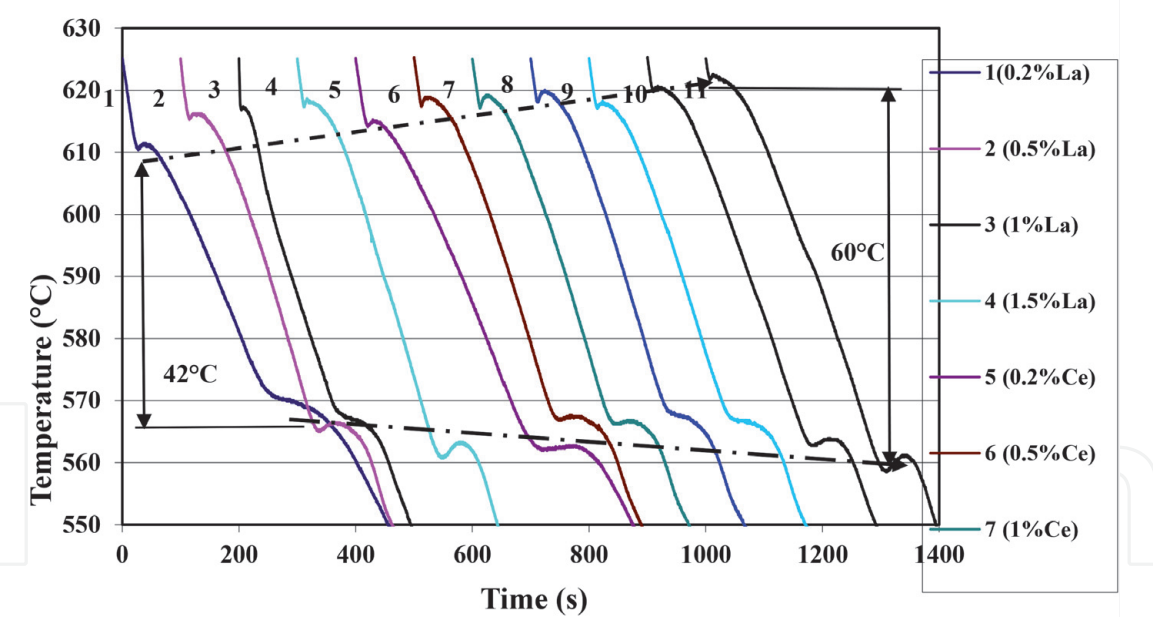


**Figure 18.**
*Solidification curves of unmodified 356 alloy [90].*

concluded that the addition of La or Ce leads only to fragmentation of the Si platelets in the case of non-modified alloys and only partial modification in the case of Sr-modified alloys. The direct advantage of the addition of RE metals to non-grained alloys is the reduction in the grain size by about 50% at 3 wt.% RE addition.

According to Song et al. [79], when RE was added to 356 alloy in the amount of 0.6 wt.%, the mean grain size was reduced by about 50%. A similar effect was observed in the work of Ibrahim et al. [91, 92] on the effect of rare earth metals on the mechanical properties of 356 and 413 alloys, as shown in **Figure 19**, in particular, in alloys 3 L and 4 L, see **Figure 19** (b, e). Due to Ce-Ti interaction, the grain refining effectiveness was reduced in the 3C and 4C alloys, as shown in **Figure 19**
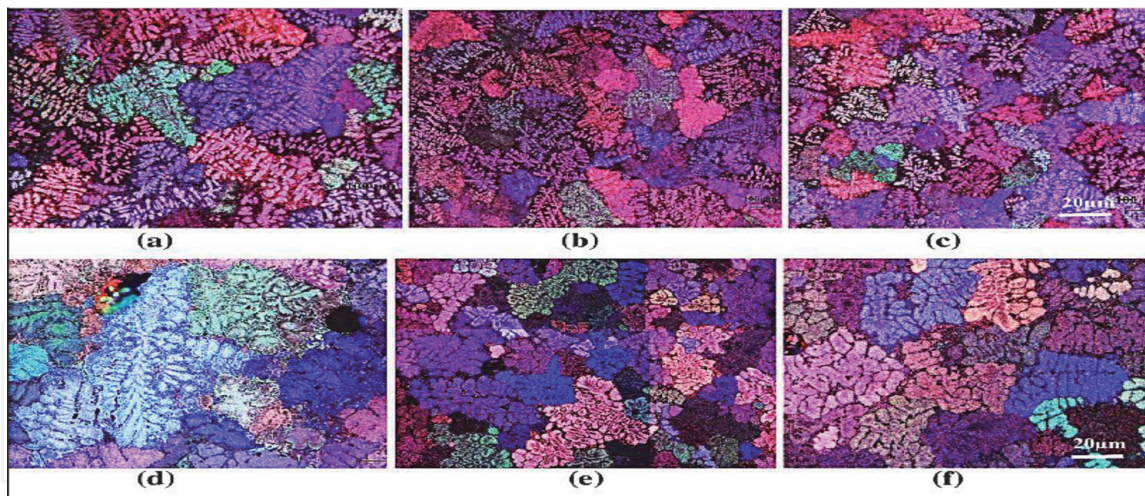
**Figure 19.**
*Effect of La and Ce addition on the grain size in A356 alloys: (a) alloy 3, no RE addition, (b) alloy 3 L, addition of 1% La, (c) alloy 3C, addition of 1% Ce. Effect of La and Ce addition on the grain size in A413 alloys: (d) alloy 4, no RE addition, (e) alloy 4 L, addition of 1% La, (f) alloy 4C, addition of 1% Ce.*

(c, f). Microstructural characterization of Al-Si cast alloys containing rare earth additions was performed by Elgallad et al. [93]. The main findings of this study were that the addition of La and/or Ce resulted in the formation of a whitecoloured Al-Si-La/Ce/(La,Ce) phase in both A356 and A413 alloys. In addition, the presence of Ti in the A356 alloy allowed for the formation of a gray-colored Al-Ti-La/Ce phase besides the Al-Si-La/Ce/(La,Ce) phase. The formation of these phases significantly increased the phase volume fraction of intermetallics in the A356 and A413 alloys. In the presence of Sr., the white-colored Al-Si-La/Ce/(La,Ce) phase was found to also contain Sr. (~1 at%). No specific Sr-La/Ce intermetallic phases were detected in the microstructures of the alloys investigated. **Figure 20** (i) shows the DSC cooling curves of the A413 alloy before and after the addition of La and Ce, individually or in combination, whereas **Figure 20** (ii) shows the DSC heating curves of the A413 alloy without and with La and/or Ce.

The results on various La additions on the microstructure of as-cast ADC12 (Al-11%Si-Cu-Mg) alloy [94] indicated that the α-Al and eutectic Si crystals were modified with the addition of 0.3 wt.% La. The eutectic Si crystals showed a granular distribution. At the same time, the alloy possessed the best mechanical properties. However, as the La addition was increased beyond 0.3 wt.%, the microstructure coarsened gradually and the mechanical properties decreased as a result.

Song et al. [77–79] analyzed the impact of different additions of La (0.0, 0.3, 0.6, and 0.9 wt.%) on the microstructure and hot crack resistance of ADC12 alloy. The results showed that, as the La added increased from 0.0% to 0.6 wt%, the structure of the α-Al phase gradually varied from a well-developed dendritic crystal into fine dendritic crystal, equiaxed crystal and spheroidal crystal; the eutectic silicon morphology varied from needle-like or tabular shape into a fine rod-like shape; the hot cracking force of the alloy also gradually decreased. Optimum alloy modification, alloy refinement and hot cracking resistance were achieved at 0.6 wt.% La addition. However, when the addition of La reached 0.9 wt.%, the excessive amount of La segregated at the grain boundaries, forming intermetallic phases.

Similarly, Chen et al. [84] evaluated the effects of combined addition of lanthanum and boron (B) on the grain refinement of Al-Si casting alloys, and found that such additions can effectively refine the grains of Al-Si alloys compared to individual addition of boron. This work also reported that with addition of La, the tensile properties of the alloy, in particular, the elongation are enhanced. The response of
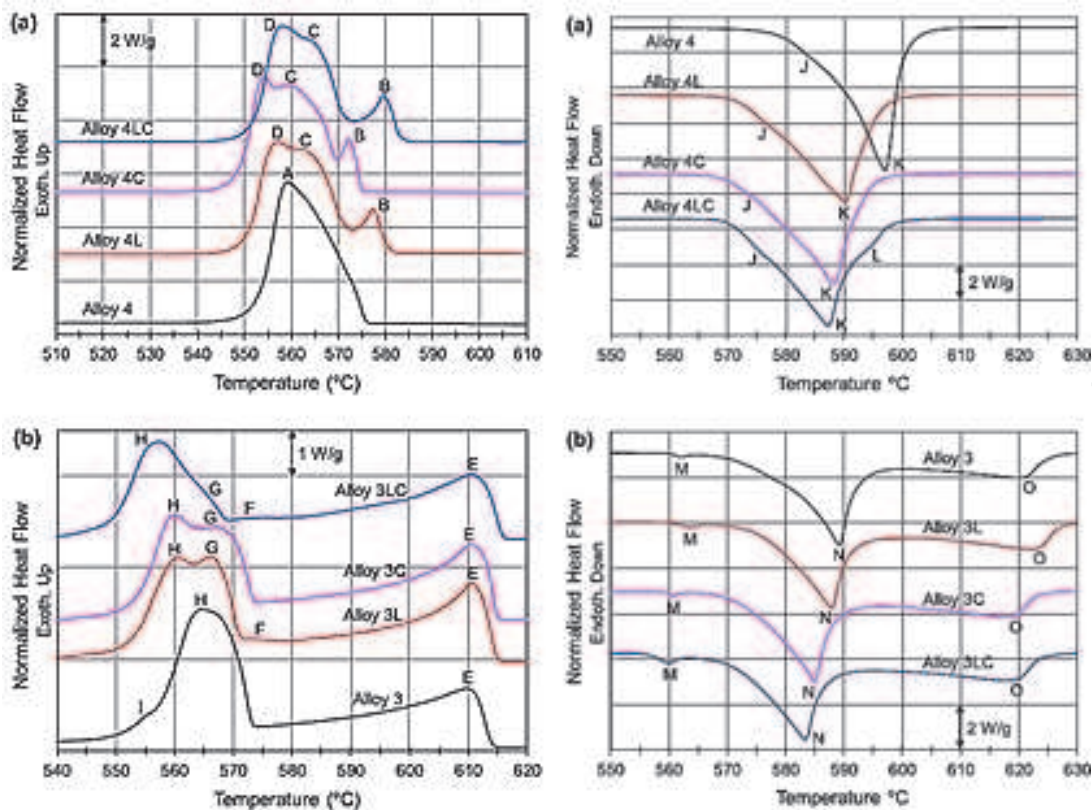
**Figure 20.**
*(i) DSC cooling curves of (a) A413 and (b) A356 alloys, respectively, without and with La and/or Ce.(ii) DSC heating curves of: (a) A413 (alloy 4) and (b) A356 (alloy 3) alloys without and with La and/or Ce [93].*

trace additions of La (0.05% - 0.1 wt.%) on the microstructures and tensile properties of B-refined and Sr-modified Al-11%Si-1.5%Cu-0.3%Mg casting alloys were investigated by Lu et al. [95] who found that introducing La/B in the weight ratio of 2:1 produced well refined α-Al grains and modified eutectic Si particles in the alloy, as well as strengthening intermetallic precipitates, which improved the ultimate tensile strength from 234 to 270 MPa, and elongation and from 4.0 to 5.8%, respectively.

A study on the synergistic effect of Sr. and La on the microstructure and mechanical properties of A356.2 alloy was carried out by Qiu et al. [96]. It was found that, with the addition of 0.5 wt.% Al-6Sr-7La master alloy, the alloy exhibited optimal microstructure and mechanical properties, with the secondary dendrite arm spacing (SDAS) decreasing to 17.9 μm and the acicular eutectic silicon transforming to a fibrous form. With the improved microstructure, the ultimate tensile strength, yield strength and elongation of the alloy (with 0.5 wt.% Al-6Sr-7La) increased to 228.15 MPa, 108.13 MPa and 11.92%, respectively, which were much better than those of the "traditionally treated" A356.2 alloy (using 0.2 wt.% Al-5Ti-1B for grain refining and 0.2 wt.% Al-10Sr for Si modification).

Tang et al. [97] investigated the effect of Sr. and La addition on the microstructure and mechanical properties of a secondary Al-Si-Cu-Fe alloy. The quantitative metallographic results indicated that addition of different levels of Sr. and La modification agents, added in the form of Al-10%Sr. and Al-10%La, produced varied refinement effects on the mean length of needle-like phases and the SDAS value. The total dosage of Sr. and La varied from 0.04 to 0.2 wt.% (Sr/La = 1:1). The minimum mean length of needle-like phases (Sr/La = 1:1) and the SDAS value (Sr/La = 1:5) were obtained by setting the addition amount of the modification agent at 0.12 wt.%. The mean length of the needle-like phase dropped from 364 to 55.3 μm, while the SDAS decreased from ~22 to 9.7 μm, i.e., by 84.5% and 55.8%, respectively.

Effect of solution treatment on the microstructure and mechanical properties of A356.2 alloy treated with Al–Sr–La master alloy was examined by Ding et al. [98] who found that the optimal solution treatment parameters for A356.2 aluminum alloy treated by Al–6Sr–7La are: solution treatment at 540 °C for 3 h, followed by quenching in 60 °C water – see **Figure 21**. The alloy under this condition possesses the optimal comprehensive conditions/values of microstructure, eutectic silicon morphology, UTS, YS, and EL, which is beneficial to the subsequent aging process.

The effects of Ti - La interaction on the microstructure and mechanical properties of B-refined and Sr-modified Al-11%Si alloys showed that the addition of 0.05 wt.% B induces a transformation of the eutectic Si from finely fibrous to coarse plate-like morphology in the Al-11%Si alloy modified with 0.02 wt% Sr., owing to the poisoning of impurity induced twinning (IIT) mechanism [99]. Thus, the eutectic Si growth occurred only by the twin plane re-entrant (TPRE) mechanism. Both Ti and La can neutralize the poisoning effect of the interaction between Sr. and B in the Al–11%Si alloy; however, the neutralizing effect of La is dependent on the addition sequence. The combined addition of La and B elements promoted the effective refinement of α-Al grains, but an inhomogeneous modification of the eutectic Si phase was also observed, leading to a slight decrease in the elongation. The poisoning effect can also be proved by the reduction of multiple Si twins as shown in **Figure 22**. **Figure 23** display the affinity of RE metals to react with Sr. leading to the observed loss of modification in the present alloys [100].

(a) 20 °C; (b) 30 °C; (c) 40 °C; (d) 50 °C; (e) 60 °C; and (f) 70 °C [98].
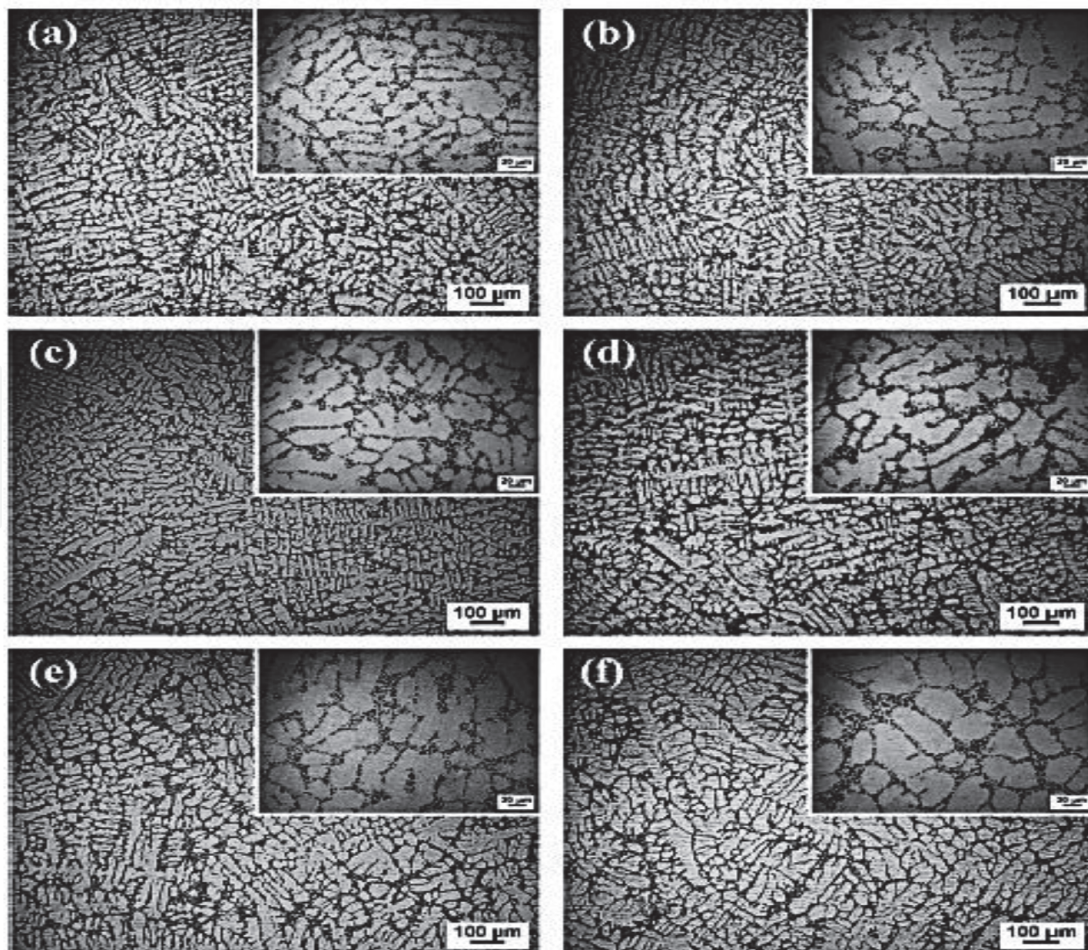


**Figure 21.**
*Effect of quenching temperatures on the microstructure of A56.2-Sr-La alloy: (a) 20 °C; (b) 30 °C; (c) 40 °C; (d) 50 °C; (e) 60 °C; and (f) 70 °C [98].*
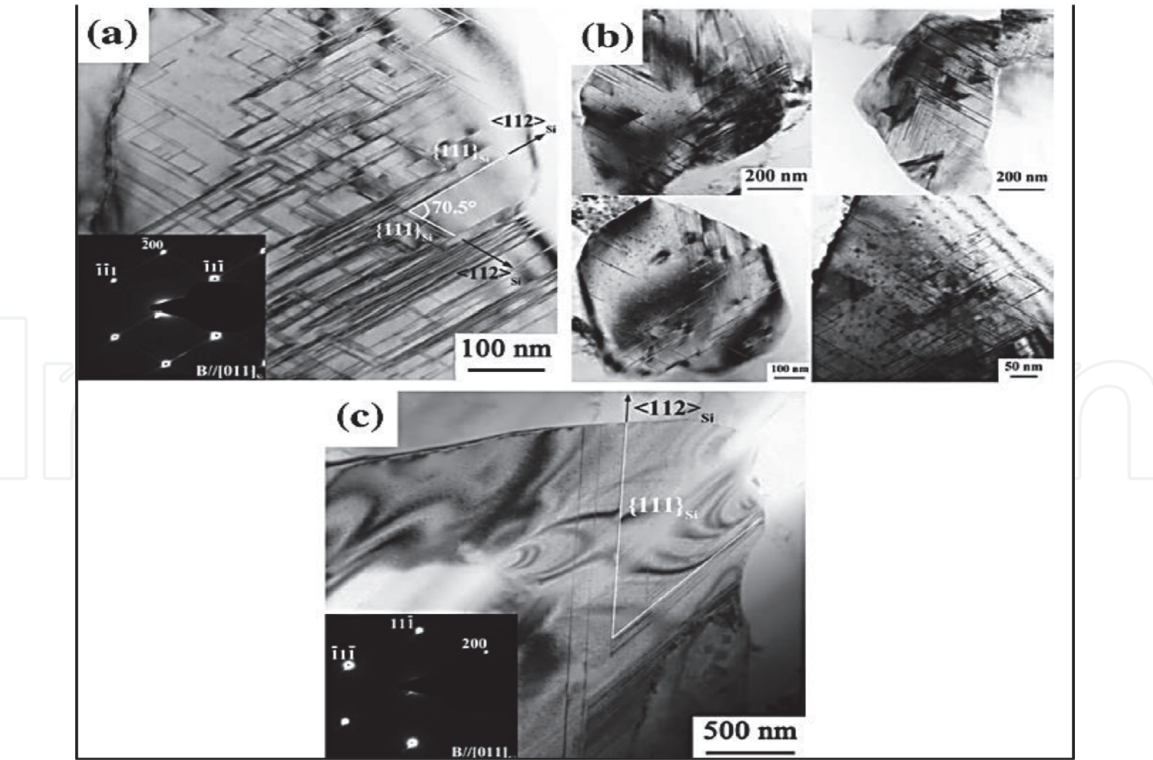
**Figure 22.**
*(a) TEM bright field image and corresponding selected area diffraction pattern of Si particle, tilted to [011]Si zone axis, in the S5 alloy (0.1216% La, 0.0526%B, 0.0218%Sr); (b) assembly of TEM bright field images of different Si particles taken from the S5 alloy; (c) TEM bright field image and corresponding selected area diffraction pattern of Si plates, tilted to [011]Si zone axis, in the S6 alloy.*
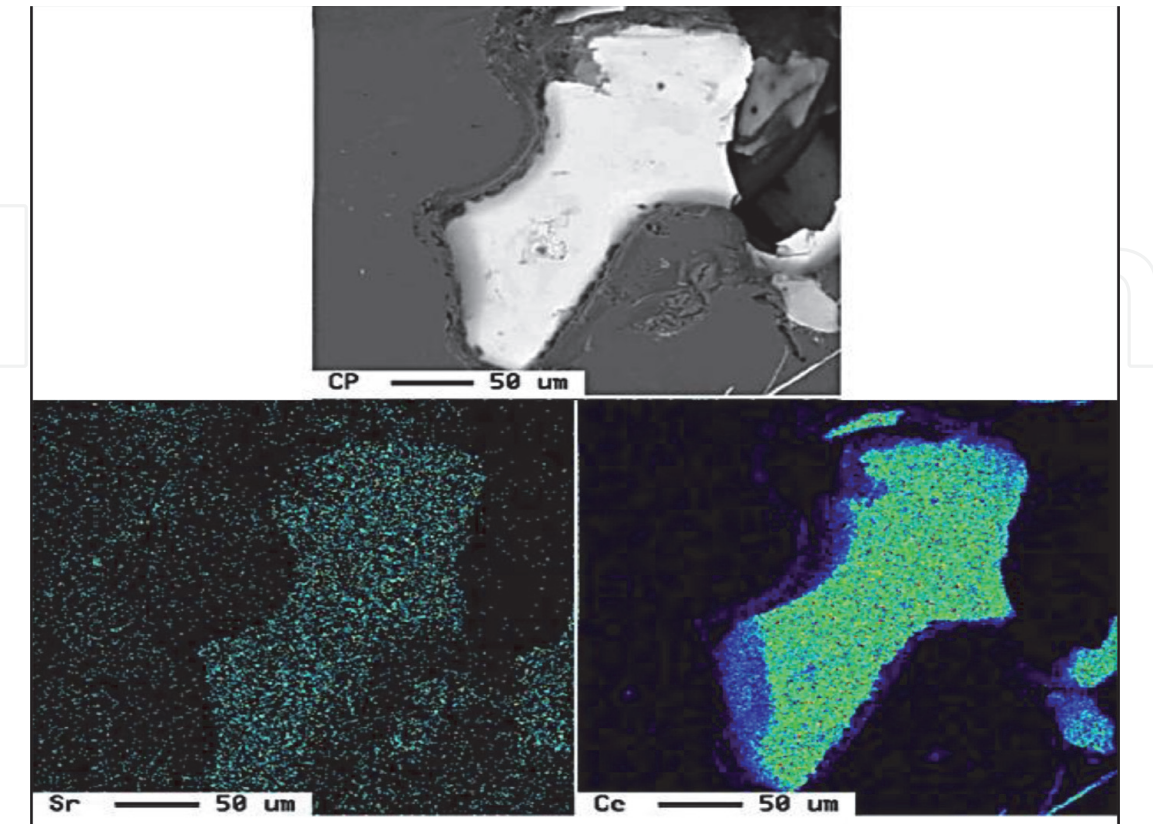


**Figure 23.**
*Ce-Sr interactions in A356 alloy modified with 1.0% Ce + 0.01% Sr. [100].*
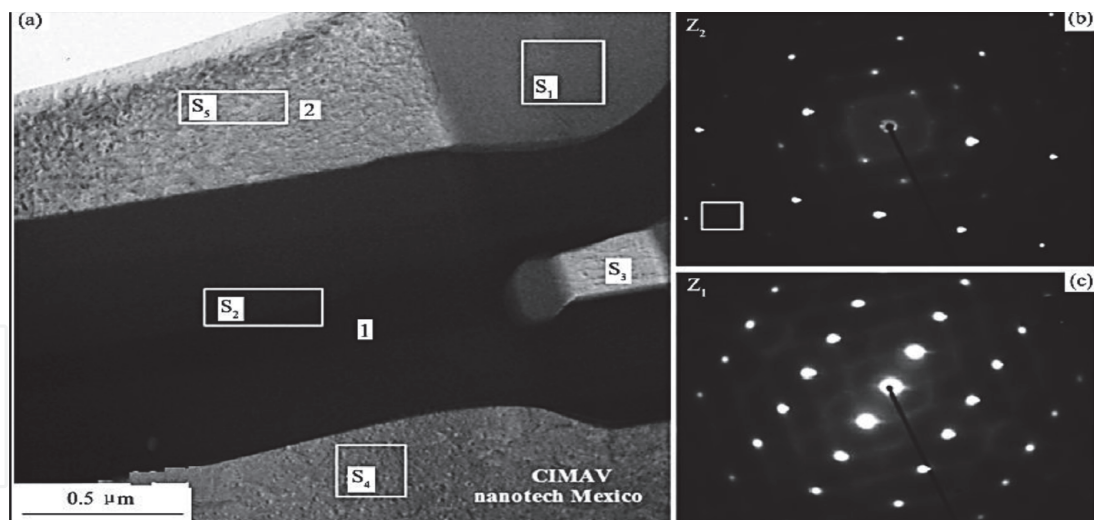
**Figure 24.**
*Bright field TEM micrograph of the La/Ce, Si and Al phases (a) squares indicate where elemental analysis was carried out; (b, c) isolated numbers indicate the zone where diffraction patterns were taken.*

## 1.4 Effects of mixed cerium and lanthanum (RE) additions

The microstructure and mechanical properties of the automotive A356 aluminum alloy reinforced with 0.2 wt.% Al-6Ce-3La (coded ACL) were investigated by Aguirre-De la Torre et al. [101]. In this study, the ACL was added to the molten A356 alloy in the as-received condition and also processed by another route, employing mechanical milling and powder metallurgy techniques. Scanning electron microscopic observations indicated a homogeneous dispersion of La/Ce phases using both routes. In regard to the mechanical properties, however, the modified A356 alloy with the ACL added in the as-received condition, showed an improvement in the mechanical performance of the A356 alloy over that reinforced with the mechanically milled ACL. A bright field TEM micrograph from the FIB-milled TEM sample is presented in **Figure 24** revealing the presence of three phases in different shades of gray as observed in **Figure 24(a)**.

Also, Wang et al. [102] studied the effects of mixed La and Ce rare earth additions on the microstructure and properties of Al-0.75%Mg-0.6%Si alloy. The results showed that the mixed addition of La and Ce had a positive effect on the grain refinement of the investigated alloy. Accordingly, the tensile strength and elongation of Al-0.75%Mg-0.6%Si alloy gradually increased with the increase in the amount of La and Ce added.

Another study was carried out by Du et al. [103–105] on the influence of 0.25 wt. % and 0.50 wt.% mixed additions of Ce and La on the microstructure and mechanical properties of an Al-Cu-Mn-Mg-Fe alloy. With the mixed addition, two intermetallic phases, $Al_8Cu_4Ce$ and $Al_6Cu_6La$, were formed. The results also showed that the 0.25 wt.% addition could promote the formation of a denser precipitation of $Al_{20}Cu_2Mn_3$ and $Al_6(Mn,Fe)$ phases, which improved the mechanical properties of the alloy at room temperature. However, up to 0.50 wt.% Ce-La addition promoted the formation of coarse $Al_8Cu_4Ce$ phase, in addition to the $Al_6Cu_6La$ and $Al_6(Mn, Fe)$ phases, which resulted in weakened mechanical properties [106, 107].

## 2. Summary

The review of the literature presented in this chapter has highlighted the numerous studies that have been carried out on the effects of rare earth elements, in

particular, Ce and La, on the microstructure and mechanical properties of aluminum alloys. While a number of these investigations have been undertaken by Chinese researchers, due likely to the easily available natural source of rare earths in the form of mischmetal, studies by other researchers are also reported. Previous studies carried out by the TAMLA research group have investigated the influence of rare earth elements and mischmetal on the performance of A356, A413.1 and other Al-Si alloys. With the more recent focus on the development of new Al-Cu based alloys for high temperature performance of automotive components, it was considered worthwhile to also investigate the effects of Ce and La rare earth metal additions to these alloys, taking into consideration low and relatively high Si levels. Putting the importance of rare earth elements into proper perspective, recently, University of Kentucky researchers have reported producing nearly pure rare earth concentrates from Kentucky coal sources [103–105]. The patent pending process developed by Honaker and Zhang is a low cost and environmentally friendly recovery process. Interest in rare earth elements is currently at its peak in the U.S.A., with the Department of Energy investing millions in research, as REs constitute essential components of diverse technologies in the high-tech and renewable energy industries.

## Appendix A- Mischmetals

| Phase no. | Element | wt-% Av. | at-% Av. | Calculated formula | Shape and color | Suggested formula |
|---|---|---|---|---|---|---|
| 1 | Al | 59.76 | 70.74 | $Al_{16}(MnFe)_4Si_3$ | Chinese script, medium gray | $Al_{15}(MnFe)_3Si_2 + \alpha.$ Iron |
| | Si | 10.07 | 11.44 | | | |
| | Fe | 20.3 | 11.6 | | | |
| | Mn | 8.31 | 4.83 | | | |
| | Total | 98.44 | 98.61 | | | |
| 2 | Al | 23.21 | 41.32 | $Al_{10}(CeLaPrNd)_4Si_9$ (Ce/La = 1.57:1) | Chinese script, white | $Al_2MM^*Si_2$† |
| | Si | 21.99 | 38.77 | | | |
| | Ce | 26.93 | 9.47 | | | |
| | La | 17.05 | 6.03 | | | |
| | Pr | 6.83 | 2.31 | | | |
| | Nd | 2.66 | 0.9 | | | |
| | Total | 98.67 | 98.8 | | | |
| 3 | Al | 22.7 | 41.06 | $Al_{10}(CeLaPrNd)_4Si_9$ (Ce/La = 1.48:1) | Chinese script, white | $Al_2MM^*Si_2$† + 0.48 wt-%Sr |
| | Si | 22.5 | 39.11 | | | |
| | Ce | 26.65 | 9.28 | | | |
| | La | 17.78 | 6.24 | | | |
| | Pr | 6.53 | 2.26 | | | |
| | Nd | 2.39 | 0.8 | | | |
| | Sr | 0.48 | 0.26 | | | |
| | Total | 99.03 | 99.01 | | | |

| Phase no. | Element | wt-% Av. | at-% Av. | Calculated formula | Shape and color | Suggested formula |
|---|---|---|---|---|---|---|
| 4 | Al | 31.02 | 52.6 | $Al_{10}(CeLaPrNd)_2(CuNi)_3Si_3$ $(Ce/La = 2.1:1)$ | Plate. like, medium light gray | $Al_5MM^*$ (CuNi) $Si^\dagger$ + excess of Al |
| | Si | 10.92 | 18.58 | | | |
| | Cu | 14.02 | 9.03 | | | |
| | Ni | 6.05 | 5.40 | | | |
| | Ce | 21.78 | 7.05 | | | |
| | La | 10.41 | 3.36 | | | |
| | Pr | 5.12 | 1.57 | | | |
| | Nd | 1.91 | 0.57 | | | |
| | Total | 101.2 | 98.16 | | | |

$^*$MM: mischmetal.
$^\dagger$Al reading could be higher than the actual content due to the small size of the examined particles.

**Table A.**
*Chemical compositions of intermetallic phases observed in as-cast A413.1 alloy containing 6 wt.% MM (WDS analysis, SDAS:120 mm) [62].*

# Appendix – B Ce addition

| Phase Color | Elements (At.%) | | | | | | Suggested phase |
|---|---|---|---|---|---|---|---|
| | Al | Ti | Fe | Cu | Si | Ce | |
| **Gray-1** | 84.41 | 6.426 | 0.025 | 2.050 | 1.526 | 4.009 | $Al_{21}Ti_2Ce$ (with trace of Cu and Si) |
| **Gray-2** | 83.08 | 6.516 | 0.052 | 2.308 | 2.726 | 4.053 | $Al_{21}Ti_2Ce$ (with trace of Cu and Si) |
| **Gray-3** | 83.88 | 6.696 | 0.015 | 1.963 | 2.278 | 4.019 | $Al_{21}Ti_2Ce$ (with trace of Cu and Si) |
| **Gray-4** | 83.66 | 6.423 | 0.013 | 2.278 | 2.331 | 3.972 | $Al_{21}Ti_2Ce$ (with trace of Cu and Si) |
| **Gray-5** | 84.60 | 6.630 | 0.025 | 1.734 | 1.872 | 4.003 | $Al_{21}Ti_2Ce$ (with trace of Cu and Si) |
| **White-1** | 40.54 | 0.000 | 0.069 | 12.38 | 26.96 | 18.58 | $Al_9Ce_4Cu_2Si_4$ |
| **White-2** | 40.44 | 0.000 | 0.069 | 11.80 | 27.73 | 18.56 | $Al_9Ce_4Cu_2Si_4$ |
| **White-3** | 46.08 | 0.000 | 0.112 | 12.04 | 24.28 | 16.52 | $Al_9Ce_4Cu_2Si_4$ |
| **White-4** | 40.21 | 0.000 | 0.122 | 12.97 | 27.04 | 18.45 | $Al_9Ce_4Cu_2Si_4$ |
| **White-5** | 40.57 | 0.000 | 0.096 | 12.24 | 26.96 | 18.78 | $Al_9Ce_4Cu_2Si_4$ |

**Table B-1.**
*WDS analysis of RE intermetallic phases observed with 1.0 wt.% Ce [70].*

| Phase Color | Elements (At.%) | | | | | | Suggested phase |
|---|---|---|---|---|---|---|---|
| | Al | Ti | Fe | Cu | Si | Ce | |
| **gray-1** | 85.78 | 6.314 | 0.014 | 1.080 | 1.388 | 4.156 | $Al_{21}Ti_2La$ (with trace of Cu and Si) |
| **gray-2** | 85.40 | 6.228 | 0.015 | 1.410 | 1.431 | 4.134 | $Al_{21}Ti_2La$ (with trace of Cu and Si) |
| **gray-3** | 84.52 | 6.255 | 0.019 | 1.777 | 1.869 | 4.265 | $Al_{21}Ti_2La$ (with trace of Cu and Si) |

| Phase Color | Elements (At.%) | | | | | | Suggested phase |
| --- | --- | --- | --- | --- | --- | --- | --- |
| | Al | Ti | Fe | Cu | Si | Ce | |
| **gray-4** | 83.99 | 6.394 | 0.008 | 2.558 | 1.601 | 4.187 | $Al_{21}Ti_2La$ (with trace of Cu and Si) |
| **gray-5** | 85.53 | 6.377 | 0.015 | 0.946 | 1.659 | 4.272 | $Al_{21}Ti_2La$ (with trace of Cu and Si) |
| **white-1** | 51.26 | 0.000 | 0.000 | 0.073 | 25.64 | 21.82 | $Al_2CeSi$ |
| **white-2** | 45.37 | 0.000 | 0.000 | 0.276 | 28.55 | 24.59 | $Al_2CeSi$ |
| **white-3** | 45.49 | 0.000 | 0.017 | 0.292 | 28.42 | 24.56 | $Al_2CeSi$ |
| **white-4** | 45.15 | 0.000 | 0.014 | 0.259 | 29.20 | 24.20 | $Al_2CeSi$ |
| **white-5** | 51.86 | 0.000 | 0.009 | 0.077 | 25.33 | 21.46 | $Al_2CeSi$ |

**Table B-2.**
*WDS analysis of RE intermetallic phases observed with 5.0 wt.% Ce [75].*

# Author details

Mohamed Gamal Mahmoud[1], Yasser Zedan[2], Agnes-Marie Samuel[3],
Victor Songmene[2], Herebert W. Doty[4] and Fawzy H. Samuel[3]*

1 Department of Mechanical Design and Production (MDP), Cairo University,
Faculty of Engineering, Egypt

2 Département de Génie Mécanique École de Technologie Supérieure, Montréal
(Qc), Canada

3 Département des Sciences Appliquées, Université du Québec à Chicoutimi,
Québec, Canada

4 Materials Technology, General Motors Global Technology Center, Warren,
MI, USA

*Address all correspondence to: fhsamuel@uqac.ca

IntechOpen

## References

[1] J. L. Murray A. J. McAlister, The Al-Si (Aluminum-Silicon) system, Bulletin of Alloy Phase Diagrams volume, 1984, 74, https://doi.org/10.1007/BF02868729.

[2] M. F. Ashby and D. R.H. Jones, in Engineering Materials 2 (Fourth Edition), 2013, Eutectic structure

[3] M. D. Sabatino and L. Arnberg, Castability of aluminium alloys, Transactions of The Indian Institute of Metals, 2009, 62, pp. 321–325

[4] G. Timelli and F. Bonollo, "Microstructure, Defects and Properties in Aluminum Alloys Castings: A Review," Proc. Int. Conf. Aluminium Two Thousand, Firenze (2007).

[5] Y.W. Lee, E. Chang, C.F. Chieu, "Modeling of Feeding Behavior of Solidifying Al-7Si-0.3Mg Alloy Plate Casting," Metall. Trans. B, 1990,21, pp. 715–722.

[6] L.H. Shang, F. Paray, J.E.Gruzleski, S. Bergeron, C. Mercadante, C.A. Loong, "Prediction of Microporosity in Al-Si Castings in Low Pressure Permanent Mould Casting Using Criteria Functions," Int. J. Cast Metals Res., 2004,17, pp. 193–200.

[7] S. Fox, and J. Campbell, "Visualisation of Oxide Film Defects During Solidification of Aluminium Alloys," Scripta Mater., 2000, 43, pp. 881–886.

[8] J. Campbell, "An Overview of the Effects of Bifilms on the Structure and Properties of Cast Alloys," Metall. And Mater. Trans. B, 2006, 37, pp. 857–863.

[9] J. Campbell and R.A. Harding, "Casting Technology,"TALAT 2.0 CD-ROM, EAA, Brussels (2000).

[10] J. Campbell, "Castings," Elsevier Science Ltd., Oxford (2003).

[11] E. Fiorese, F. Bonollo, G. Timelli, L. Arnberg, E. Gariboldi, NEW CLASSIFICATION OF DEFECTS AND IMPERFECTIONS FOR ALUMINUM ALLOY CASTINGS, International Journal of Metalcasting, 2015, 9, pp. 55–66.

[12] J. Campbell, "Materials Perspective, Entrainment Defects," Mater. Sci. Technol., 2006, 22, pp. 132–136.

[13] John Campbell, in Complete Casting Handbook (Second Edition), 2015.

[14] Aluminum: Properties and Physical Metallurgy Editor: John E. Hatch, ASM International, ISBN: 978–0–87170-176-3.

[15] K.Gupta, D.J.Lloyd, S.A.Court, Precipitation hardening in Al–Mg–Si alloys with and without excess Si, Materials Science and Engineering: A , 2001, 316, pp.11–17.

[16] H. Liao, Y. Wu, K. Ding, Materials Science and Engineering A, 2013, 560, pp.811–816.

[17] Aluminum Casting Technology, American Foundrymen<s Society, inc., Des Plains, Il, 1986.

[18] Y.F. Ye, Q. Wang, J. Lu, C.T. Liu and Y. Yang, High-entropy alloy: challenges and prospects, Materials Today, 2016, 19, pp. 349–362.

[19] E. J. Pickering and N. G. Jones, High-entropy alloys: a critical assessment of their founding principles and future prospects, International Materials Reviews, 2016, 61, pp. 183–202.

[20] Knuutinen, A., et al., Modification of Al–Si alloys with Ba, Ca, Y and Yb. Journal of Light Metals, 2001. 1(4): p. 229–240.

[21] Nogita, K., et al., Mechanisms of eutectic solidification in Al–Si alloys

modified with Ba, Ca, Y and Yb. Journal of light metals, 2001. 1(4): p. 219–228.

[22] Li, B., F. Kong, and Y. Chen, Effect of yttrium addition on microstructures and room temperature tensile properties of Ti-47 Al alloy. Journal of rare earths, 2006. 24(3): p. 352–356.

[23] Li, H.Z., et al., Effect of Y content on microstructure and mechanical properties of 2519 aluminum alloy. Transactions of Nonferrous Metals Society of China, 2007. 17(6): p. 1194–1198.

[24] Zheng, L. and H. Yongmei, Effect of yttrium on the microstructure of a semi-solid A356 Al alloy. Rare Metals, 2008. 27(5): p. 536–540.

[25] Sheng, M., et al., Effects of Y and Y combined with Al-5Ti-1B on the microstructure and mechanical properties of hypoeutectic Al-Si alloy. JOM, 2015. 67(2): p. 330–335.

[26] Nie, Z.R., et al. Research on rare earth in aluminum. in Materials Science Forum. 2002. Trans Tech Publ.

[27] Nie, Z., et al. Advanced aluminum alloys containing rare-earth erbium. in Materials Forum. 2004.

[28] Xu, G.F., et al., Effect of trace rare earth element Er on Al-Zn-Mg alloy. Transactions of Nonferrous Metals Society of China, 2006. 16(3): p. 598–603.

[29] Li, Y.T., et al. Alloying behavior of rare-earth Er in Al-Cu-Mg-Ag alloy. in Materials science forum. 2007. Trans Tech Publ.

[30] Wen, S.P., et al., The effect of erbium on the microstructure and mechanical properties of Al-Mg-Mn-Zr alloy. Materials Science and Engineering a-Structural Materials Properties Microstructure and Processing, 2009. 516(1–2): p. 42–49.

[31] Colombo, M., E. Gariboldi, and A. Morri, Er addition to Al-Si-Mg-based casting alloy: Effects on microstructure, room and high temperature mechanical properties. Journal of Alloys and Compounds, 2017. 708: p. 1234–1244.

[32] Colombo, M., E. Gariboldi, and A. Morri, Influences of different Zr additions on the microstructure, room and high temperature mechanical properties of an Al-7Si-0.4 Mg alloy modified with 0.25% Er. Materials Science and Engineering: A, 2017.

[33] Li, Q.L., et al. Effect of Rare Earth Er on Microstructure and Mechanical Properties of Cast Al-Si-Mg Alloy. in Materials Science Forum. 2017. Trans Tech Publ.

[34] Xu, C., et al., Effect of Al–P–Ti–TiC–Nd 2 O 3 modifier on the microstructure and mechanical properties of hypereutectic Al–20wt.% Si alloy. Materials Science and Engineering: A, 2007. 452: p. 341–346.

[35] Shi, W.X., et al., Effect of Nd on microstructure and wear resistance of hypereutectic Al-20%Si alloy. Journal of Alloys and Compounds, 2010. 508(2): p. 480–485.

[36] Weixi, S., et al., Effect of neodymium on primary silicon and mechanical properties of hypereutectic Al-15% Si alloy. Journal of Rare Earths, 2010. 28: p. 367–370.

[37] Ren, X., et al., Effect of Nd on microstructure and properties of 2A70 alloy. Journal of Alloys and Compounds, 2017.

[38] Tang, Q., et al., The effects of neodymium addition on the intermetallic microstructure and mechanical properties of Al-7Si-0.3 Mg-0.3 Fe alloys. Journal of Alloys and Compounds, 2018.

[39] Ahmad, R., M. Asmael, and M. Amzar, Effect of ytterbium addition on

microstructure and hardness of Al-6.5Si-1Zn secondary cast alloy. 2006.

[40] Xiao, D., et al., Effect of rare earth Yb addition on mechanical properties of Al–5· 3Cu–0· 8Mg–0· 6 Ag alloy. Materials science and technology, 2007. 23(10): p. 1156–1160.

[41] Zhang, X.M., et al., Effects of Yb addition on microstructures and mechanical properties of 2519A aluminum alloy plate. Transactions of Nonferrous Metals Society of China, 2010. 20(5): p. 727–731.

[42] Li, B., et al., Microstructure evolution and modification mechanism of the ytterbium modified Al-7.5%Si-0.45%Mg alloys. Journal of Alloys and Compounds, 2011. 509(7): p. 3387–3392.

[43] Li, J.H., et al., Refinement of Eutectic Si Phase in Al-5Si Alloys with Yb Additions. Metallurgical and Materials Transactions a-Physical Metallurgy and Materials Science, 2013. 44a(2): p. 669–681.

[44] Hu, Z., et al., Solidification behavior, microstructure and silicon twinning of Al-10Si alloys with Yb addition. Journal of Rare Earths, 2018.

[45] Li, Q., et al., Mechanical Properties and Microstructural Evolution of Yb-Modified Al-20% Si Alloy. Journal of Materials Engineering and Performance, 2018: p. 1–10.

[46] Nogita, K., S.D. McDonald, and A. K. Dahle, Eutectic modification of Al-Si alloys with rare earth metals. Materials Transactions, 2004. 45(2): p. 323–326.

[47] Chen, Z.W., P. Chen, and C.Y. Ma, Microstructures and mechanical properties of Al-Cu-Mn alloy with La and Sm addition. Rare Metals, 2012. 31 (4): p. 332–335.

[48] Qiu, H., H. Yan, and Z. Hu, Effect of samarium (Sm) addition on the

microstructures and mechanical properties of Al–7Si–0.7 Mg alloys. Journal of Alloys and Compounds, 2013. 567: p. 77–81.

[49] Zhang, W., et al., Effects of Sc content on the microstructure of As-Cast Al-7wt.% Si alloys. Materials Characterization, 2012. 66: p. 104–110.

[50] Patakham, U., J. Kajornchaiyakul, and C. Limmaneevichitr, Modification mechanism of eutectic silicon in Al–6Si–0.3 Mg alloy with scandium. Journal of Alloys and Compounds, 2013. 575: p. 273–284.

[51] C. Y. Young, L. Qingchaun, and J. Zhuling, "Influence of cerium and mischmetal on the hardness and brightness of Al-Mg-Si alloys," Journal of the Less Common Metals, vol. 110, 1985, pp. 175–178.

[52] M. Ravi, U. T. S. Pillai, B. C. Pai, A. D. Damodaran, and E. S. Dwarakadasa, "A study of the influence of mischmetal additions to ai-7si-0.3 mg (lm 25/356) alloy," Metallurgical and Materials Transactions A, vol. 27, 1996, pp. 1283–1292.

[53] Chang, J.Y., et al., Rare earth concentration in the primary Si crystal in rare earth added Al-21wt.%Si alloy. Scripta Materialia, 1998. 39(3): p. 307–314.

[54] Chang, J.Y., I.G. Moon, and C.S. Choi, Refinement of cast microstructure of hypereutectic Al-Si alloys through the addition of rare earth metals. Journal of Materials Science, 1998. 33(20): p. 5015–5023.

[55] Li, J.H., et al., Modification of eutectic Si in Al-Si alloys with Eu addition. Acta Materialia, 2015. 84: p. 153–163.

[56] Mao, F., et al., The interaction between Eu and P in high purity Al-7Si

alloys. Materials Characterization, 2016. 120: p. 129–142.

[57] Ravi, M., et al., The effect of mischmetal addition on the structure and mechanical properties of a cast Al-7Si-0.3 Mg alloy containing excess iron (up to 0.6 Pct). Metallurgical and Materials Transactions A, 2002. 33(2): p. 391–400.

[58] Weiwei, W.A.N., et al., Study of rare earth element effect on microstructures and mechanical properties of an Al-Cu-Mg-Si cast alloy. Rare Metals, 2006. 25(6): p. 129–132.

[59] Chong, C., et al., Influences of complex modification of P and RE on microstructure and mechanical properties of hypereutectic Al-20Si alloy. Transactions of Nonferrous Metals Society of China, 2007. 17(2): p. 301–306.

[60] El Sebaie, O., et al., The effects of mischmetal, cooling rate and heat treatment on the hardness of A319. 1, A356. 2 and A413. 1 Al–Si casting alloys. Materials Science and Engineering: A, 2008. 486(1): p. 241–252.

[61] El Sebaie , O., et al., The effects of mischmetal, cooling rate and heat treatment on the eutectic Si particle characteristics of A319.1, A356.2 and A413.1 Al–Si casting alloys. Materials Science and Engineering: A, 2008. 480 (1–2): p. 342–355.

[62] Elsebaie, O., F.H. Samuel, and S. Al Kahtani, Intermetallic phases observed in non-modified and Sr modified Al-Si cast alloys containing mischmetal. International Journal of Cast Metals Research, 2013. 26(1): p. 1–15.

[63] Doty, H.W., S.A. Alkahtani, O. Elsebaie and F.H. Samuel, Influence of Metallurgical Parameters on the Impact Toughness of Near Eutectic Al-Si Alloys, in 119th Metalcasting Congress, AFS 2015, Columbus, OH, April 21–23, 2015.

2015, American Foundry Society: Columbus, Ohio.

[64] El Sebaie, O., The Effect of Mischmetal, Cooling Rate and Heat Treatment on the Microstructure and Hardness of 319, 356, and 413 Aluminum-silicon Alloys. 2006, UQAC.

[65] Li, Y.G., et al., Effect of co-addition of RE, Fe and Mn on the microstructure and performance of A390 alloy. Materials Science and Engineering a-Structural Materials Properties Microstructure and Processing, 2009. 527(1–2): p. 146–149.

[66] Zhu, M., et al., Effect of mischmetal modification treatment on the microstructure, tensile properties, and fracture behavior of Al-7.0%Si-0.3%Mg foundry aluminum alloys. Journal of Materials Science, 2011. 46(8): p. 2685–2694.

[67] Zhu, M., et al., Effects of T6 heat treatment on the microstructure, tensile properties, and fracture behavior of the modified A356 alloys. Materials & Design, 2012. 36: p. 243–249.

[68] Mousavi, G.S., M. Emamy, and J. Rassizadehghani, The effect of mischmetal and heat treatment on the microstructure and tensile properties of A357 Al-Si casting alloy. Materials Science and Engineering a-Structural Materials Properties Microstructure and Processing, 2012. 556: p. 573–581.

[69] Mahmoud, M.G., et al., Effect of Solidification Rate and Rare Earth Metal Addition on the Microstructural Characteristics and Porosity Formation in A356 Alloy. Advances in Materials Science and Engineering, 2017: p. 1–15.

[70] Mahmoud, M.G., et al., Effect of Rare Earth Metals, Sr, and Ti Addition on the Microstructural Characterization of A413.1 Alloy. Advances in Materials Science and Engineering, 2017. 2017.

[71] Jiang, W.M., et al., Effects of rare earth elements addition on microstructures, tensile properties and fractography of A357 alloy. Materials Science and Engineering a-Structural Materials Properties Microstructure and Processing, 2014. 597: p. 237–244.

[72] Zhang, J., et al., Microstructural development of Al–15wt.% Mg 2 Si in situ composite with mischmetal addition. Materials Science and Engineering: A, 2000. 281(1): p. 104–112.

[73] Zhang, H.R., et al., Cooling Rate Sensitivity of RE-Containing Grain Refiner and Its Impact on the Microstructure and Mechanical Properties of A356 Alloy. Acta Metallurgica Sinica-English Letters, 2016. 29(5): p. 414–421.

[74] Dang, B., Z.Y. Jian, and J.F. Xu, Effects of rare-earth element addition and heat treatment on the microstructures and mechanical properties of Al-25% Si alloy. International Journal of Materials Research, 2017. 108(4): p. 269–274.

[75] Mahmoud, M.G., A.M. Samuel, H. W. Doty and F.H. Samuel, *Role of Heat Treatment on the Tensile Properties and Fractography of Al–1.2Si–2.4Cu and Al–8.0Si–2.4Cu Cast Alloys Modified with Ce, La and Sr Addition.* International Journal of Metalcasting, 2020. **14**(1): p. 218–242.

[76] Mahmoud, M.G., A.M. Samuel, H. W. Doty and F.H. Samuel, *Effect of the Addition of La and Ce on the Solidification Behavior of Al–Cu and Al–Si–Cu Cast Alloys.* International Journal of Metalcasting, 2020. **14**(1): p. 191–206.

[77] Song, M., K.H. Chen, and L.P. Huang, Effects of Ce and Ti on the microstructures and mechanical properties of an Al-Cu-Mg-Ag alloy. Rare Metals, 2007. 26(1): p. 28–32.

[78] Song, M., D.H. Xiao, and F.Q. Zhang, Effect of Ce on the thermal stability of the Omega phase in an Al-Cu-Mg-Ag alloy. Rare Metals, 2009. 28 (2): p. 156–159.

[79] Song, X.C., H. Yan, and F.H. Chen, Impact of Rare Earth Element La on Microstructure and Hot Crack Resistance of ADC12 Alloy. Journal of Wuhan University of Technology-Materials Science Edition, 2018. 33(1): p. 193–197.

[80] Xiao, D.H., J.N. Wang, and D.Y. Ding, Effect of minor cerium additions on microstructure and mechanical properties of cast Al – Cu – Mg – Ag alloy. Materials Science and Technology, 2004. 20(10): p. 1237–1240.

[81] Voncina, M., et al., Effect of Ce on solidification and mechanical properties of A360 alloy. Journal of Alloys and Compounds, 2011. 509(27): p. 7349–7355.

[82] Voncina, M., et al., Microstructure and grain refining performance of Ce on A380 alloy. Journal of Mining and Metallurgy, Section B: Metallurgy, 2012. 48(2): p. 265–272.

[83] Chen, Z.W., et al., Kinetic nucleation of primary alpha (Al) dendrites in Al-7%Si-Mg cast alloys with Ce and Sr additions. Transactions of Nonferrous Metals Society of China, 2013. 23(12): p. 3561–3567.

[84] Chen, Y., et al., Effects of combinative addition of lanthanum and boron on grain refinement of Al-Si casting alloys. Materials & Design, 2014. 64: p. 423–426.

[85] Ye, L.Y., et al., Influence of Ce addition on impact properties and microstructures of 2519A aluminum alloy. Materials Science and Engineering: A, 2013. 582: p. 84–90.

[86] Yii, S.L. & Norazman, Anas & Nasir, Ramdziah & Anasyida, A.S..

(2016). Microstructural and Mechanical Properties of Al-20%Si Containing Cerium. Procedia Chemistry. 19. 304–310. 10.1016/j.proche.2016.03.015.

[87] Ahmad, R. and M.B.A. Asmael, Influence of Cerium on Microstructure and Solidification of Eutectic Al–Si Piston Alloy. Materials and Manufacturing Processes, 2015. 31(15): p. 1948–1957.

[88] Ahmad, R., et al., Reduction in secondary dendrite arm spacing in cast eutectic Al–Si piston alloys by cerium addition. International Journal of Minerals, Metallurgy, and Materials, 2017. 24(1): p. 91–101.

[89] Mahmoud, M.G., A.M. Samuel, H. W. Doty and F.H. Samuel, *Formation of Rare Earth Intermetallics in Al–Cu Cast Alloys*, in *Light Metals Symposium held at the 149th Annual Meeting and Exhibition, TMS 2020, 23 February 2020 through 27 February 2020*. 2020: San Diego; United States. p. 241–246.

[90] Mahmoud, M.G., E.M. Elgallad, M. F. Ibrahim and F.H. Samuel, *Effect of Rare Earth Metals on Porosity Formation in A356 Alloy.* International Journal of Metalcasting, 2018. **12**(2): p. 251–265.

[91] Ibrahim, M.F., M.H. Abdelaziz, A. M. Samuel, H.W. Doty and F.H. Samuel, *Effect of Rare Earth Metals on the Mechanical Properties and Fractography of Al–Si-Based Alloys.* International Journal of Metalcasting, 2020. **14**(1): p. 108–124.

[92] Ibrahim, A.I., E.M. Elgallad, A.M. Samuel, H.W. Doty and F.H. Samuel, *Effects of heat treatment and testing temperature on the tensile properties of Al–Cu and Al–Cu–Si based alloys.* International Journal of Materials Research, 2018. **109**(4): p. 314–331.

[93] Elgallad, E.M., M.F. Ibrahim, H.W. Doty and F.H. Samuel, *Microstructural characterisation of Al–Si cast alloys containing rare earth additions.* Philosophical Magazine, 2018. **98**(15): p. 1337–1359.

[94] Huang, X. and H. Yan, Effect of trace La addition on the microstructure and mechanical property of as-cast ADC12 Al-Alloy. Journal of Wuhan University of Technology-Materials Science Edition, 2013. 28(1): p. 202–205.

[95] Lu, T., et al., Effects of La addition on the microstructure and tensile properties of Al-Si-Cu-Mg casting alloys. International Journal of Minerals Metallurgy and Materials, 2015. 22(4): p. 405–410.

[96] Qiu, C., et al., Synergistic effect of Sr and La on the microstructure and mechanical properties of A356. 2 alloy. Materials & Design, 2016.

[97] Tang, P., et al., Influence of strontium and lanthanum simultaneous addition on microstructure and mechanical properties of the secondary Al-Si-Cu-Fe alloy. Journal of Rare Earths, 2017. 35(5): p. 485–493.

[98] Ding, J., et al., Effect of Solution Treatment on Microstructure and Mechanical Properties of A356. 2 Aluminum Alloy Treated With Al–Sr–La Master Alloy. Advanced Engineering Materials, 2018.

[99] Li, C., et al., Effects of Ti and La Additions on the Microstructures and Mechanical Properties of B-Refined and Sr-Modified Al–11Si Alloys. Metals and Materials International, 2018: p. 1–10.

[100] Alkahtani, S.A., E.M. Elgallad, M. M. Tash, A.M. Samuel and F.H. Samuel, Effect of rare earth metals on the microstructure ao AL-SI based alloys. Materials, 2017. **9**(1).

[101] Aguirre-De la Torre, E., et al., Mechanical properties of the A356 aluminum alloy modified with La/Ce.

Journal of Rare Earths, 2013. 31(8): p. 811–816.

[102] Wang, S.C., et al. Effects of La and Ce Mixed Rare Earth on Microstructure and Properties of Al-Mg-Si Aluminum Alloy. in Materials Science Forum. 2017. Trans Tech Publ.

[103] Du, J.D., et al., Effect of CeLa addition on the microstructures and mechanical properties of Al-Cu-Mn-Mg-Fe alloy. Materials Characterization, 2017. 123: p. 42–50.

[104] UK Researchers First to Produce High Grade Rare Earths From Coal: @universityofky; 2017 [updated 2017-11-20. Available from: https://uknow.uky.edu/research/uk-researchers-first-produce-high-grade-rare-earths-coal

[105] Mao, F., et al., Effect of Eu addition on the microstructures and mechanical properties of A356 aluminum alloys. Journal of Alloys and Compounds, 2015. 650: p. 896–906.

[106] Tzeng, Y.-C., et al., Effects of scandium addition on iron-bearing phases and tensile properties of Al–7Si–0.6 Mg alloys. Materials Science and Engineering: A, 2014. 593: p. 103–110.

[107] Xu, C., et al., The synergic effects of Sc and Zr on the microstructure and mechanical properties of Al-Si-Mg alloy. Materials & Design, 2015. 88: p. 485–492.